Iron and Ruthenium Alkynyl Complexes with 2-Fluorenyl Groups: Some Linear and Nonlinear Optical Absorption Properties

F. Malvolti, C. Rouxel, G. Grelaud, Loic Toupet, T. Roisnel, A. Barlow, X. Yang, Gang Wang, F.I. Abdul Razak, R. Stranger, et al.

Iron and Ruthenium Alkynyl Complexes with 2-Fluorenyl Groups: Some Linear and Nonlinear Optical Absorption Properties

Floriane Malvolti,[a] Cedric Rouxel,[a] Guillaume Grelaud,[a,b] Loic Toupet,[c] Thierry Roisnel,[a] Adam Barlow,[b] Fazira I. Abdul Razak,[b] Robert Stranger,[b] Marie P. Cifuentes,[b] Mark G. Humphrey,[b]* Olivier Mongin,[a] Mireille Blanchard-Desce,[d] Christine Paul-Roth[a] and Frédéric Paul[a]*

Abstract: Four new mononuclear alkynyl complexes featuring a terminal 2-fluorenyl group, namely Fe(η^5-C_5Me_5)$(CO)_2$[C≡C(2-$C_{21}H_{25}$)] (**2**), Ru(κ^2-dppe)$_2$(Cl)[C≡C(2-$C_{21}H_{25}$)] (**3**), Ru(κ^2-dppe)$_2$[C≡C(4-$C_6H_4NO_2$)][C≡C(2-$C_{21}H_{25}$)] (**4**), and [Fe(η^5-C_5Me_5)(κ^2-dppe){C≡C(C_5H_4N)-CH_2(2-$C_{13}H_9$)}][PF_6] (**5**[PF_6]), have been synthesized and characterized and their redox, absorption and emission properties have been studied. For the two ruthenium derivatives (**3**-**4**), these studies are complemented by spectroelectrochemical investigations, Z-scan measurements and DFT calculations. Fluorimetric studies reveal that these compounds are poorly or not luminescent, and, when luminescent, that the weak luminescence detected most likely originates from a higher lying (LC) excited state presumably located on fluorene. Finally, the third-order NLO properties of **3** and **4** are reported. It is shown that the bis-alkynyl complex **4** is significantly more active than **3** and that both compounds exhibit two-photon absorption (TPA) around 860-1050 nm, with TPA cross-sections above 350 GM. In addition, it is shown that both species should give rise to a marked switching of their cubic nonlinear optical (NLO) properties in this spectral range upon oxidation.

Introduction

Inorganic or organometallic photo-active molecules presenting facile electron-transfer capabilities have attracted sustained interest in diverse fields ranging from photovoltaic conversion to electroluminescent displays[1] for more than forty years.[2] Among them, redox-active iron(II) or ruthenium(II) alkynyl complexes were identified very early as outstanding electrophores.[3] These species, which were initially demonstrated to constitute key building blocks for molecular electronics,[3f,4] have revealed more recently a very promising potential in molecular photonics,[5] largely attributable to their remarkable electrochromism,[6] which extends to their nonlinear optical (NLO) properties.[7] So far, however, only a handful of investigations have been concerned with their luminescence.[8] The latter appears usually to be weak or non-existent, even when a good luminophore is incorporated into the alkynyl ligand.[8b,8e,f,9] This is regrettable, since luminescence, in association with the large cubic NLO properties exhibited by some of these compounds (notably two-photon absorption), would constitute a highly attractive feature that would significantly enlarge the applied scope of these molecules.[10]

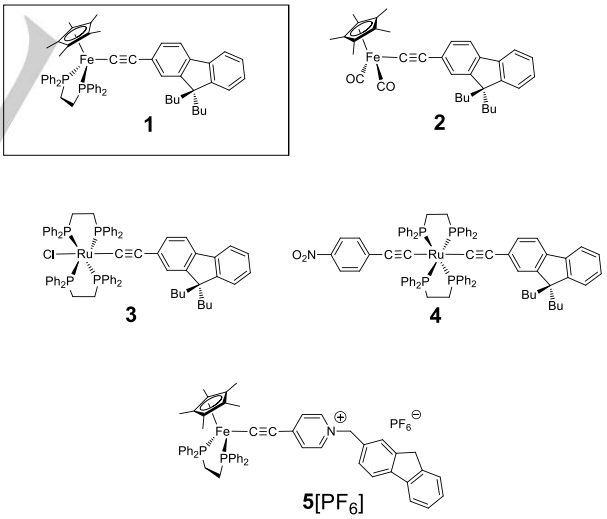

Scheme 1. Selected Alkynyl Complexes Containing *9H*-Fluorenyl Units.

In this context, we have recently reported a series of [Fe(η^5-C_5Me_5)(κ^2-dppe)]-based organoiron complexes containing 2-ethynylfluorenyl ligands such as **1** (Scheme 1), which present strong (and redox-switchable) third-order NLO activities around 800 nm.[11] Remarkably, when excited around 300 nm, these Fe(II) chromophores are weakly emissive, but not from their first excited state, with luminescence quantum yields around a few percent (0.4 % for **1**). In line with previous proposals in the

[a] Dr F. Malvolti, Dr C. Rouxel, Dr. G. Grelaud, T. Roisnel, Dr O. Mongin, Dr C. Paul-Roth, Dr F. Paul
Institut des Sciences Chimiques de Rennes, CNRS (UMR 6226)
Université de Rennes 1
Campus de Beaulieu, 35042 Rennes Cedex (France)
Tel: (+33) 02-23-23-59-62
E-mail: frederic.paul@univ-rennes1.fr
[b] Dr. G. Grelaud, Dr. A. Barlow, Dr. F. I. Abdul Razak, Em. Prof. R. Stranger, Assoc. Prof. M. P. Cifuentes, Prof. M. G. Humphrey
Research School of Chemistry, Australian National University
Canberra, ACT 2601 (Australia)
Tel: (+61) 2-61252927
E-mail: mark.humphrey@anu.edu.au
[c] Dr. L. Toupet
Institut de Physique de Rennes (IPR), CNRS (UMR 6251)
Université de Rennes 1
Campus de Beaulieu, 35042 Rennes Cedex (France)
[d] Dr. M. Blanchard-Desce
ISM, CNRS (UMR 5255)
Université Bordeaux
33400 Talence (France)

Supporting information for this article is given via a link at the end of the document.

literature,[8c,8e,f] a redox trapping mechanism of the photogenerated fluorene-centred (LC) excited state can be tentatively proposed to rationalize their weak and unusual fluorescence (Scheme 2). This proposal, which rests on the statement that Fe(II) endgroups can be readily oxidized (and reduced with considerable difficulty), has however not been experimentally challenged so far.

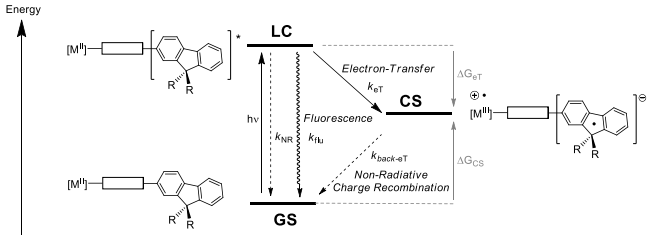

Scheme 2. Proposed Redox-Trapping Mechanism of the Fluorene-Based Luminescence in 2-Ethynylfluorenyl Complexes such as **1**.

According to Marcus theory,[12] the rate (k_{eT}) of any photoinduced electron transfer process should be strongly influenced by the redox potentials of the redox-active sites experiencing this electron transfer. Based on eq. 1, the detection of some luminescence indicates that the non-radiative decay (k_{eT} + k_{NR}) does not completely overcome the radiative decay (k_{lum}) in these alkynyl complexes. If the rate of the oxidative quenching process (k_{eT}) dominates the rates of the other non-radiative deactivation processes (k_{eT} >> k_{NR}), the non-radiative decay should be controlled by the oxidation potential of the d^6 transition metal center. Changing this potential could improve the luminescence of these species. We therefore decided to measure the luminescence of selected 2-ethynyl-9,9-dibutylfluorenyl complexes with higher oxidation potentials than **1**, such as **2**-**4** (Scheme 1), hoping that such species would be more luminescent than **1**. In addition, Z-scan investigations should reveal how the nature and redox potential of the d^6 metal center influence their third-order NLO properties. Finally, to probe the influence of the spacer between the metal center and the fluorene luminophore on the quenching process, this series was complemented by **5**[PF_6], a cationic Fe(II) compound incorporating the *9H*-fluorenyl group as a side-group, i.e. not π-conjugated with the metal center.

$$\Phi_{lum} = k_{lum}/(k_{lum} + k_{eT} + k_{NR}) \qquad (1)$$

We thus report hereafter (i) the synthesis and characterization of the new complexes **2**, **3**, **4** and **5**[PF_6], (ii) selected linear and nonlinear optical properties for some of these species, and (iii) the results of spectroelectrochemical investigations specifically conducted on the Ru(II) derivatives **2** and **3**. These data will be compared to those of **1** and discussed with the help of DFT calculations, a particular emphasis being placed on (i) establishing (or not) the occurrence of a reductive-trapping mechanism of the fluorene-based luminescence (Scheme 2) and on (ii) determining the influence of the metal center and spacer structure on the third-order NLO properties of such 2-ethynylfluorenyl complexes.

Results and Discussion

Synthesis and Characterization of the Fe(II) Carbonyl Complex 2. The synthesis of the Fe(II) alkynyl complex **2** was effected from the known Fe(II) bis-carbonyl chloride precursor **6** and the organic 2-alkynyl-9,9-dibutyl-*9H*-fluorene (**7**) previously reported,[11] following a workup recently developed in our group (Scheme 3). Due to the very high solubility of this complex in common organic solvents most of the product was lost during the purification procedure. This complicated seriously its isolation in pure form and resulted in a rather low yield (31 %).

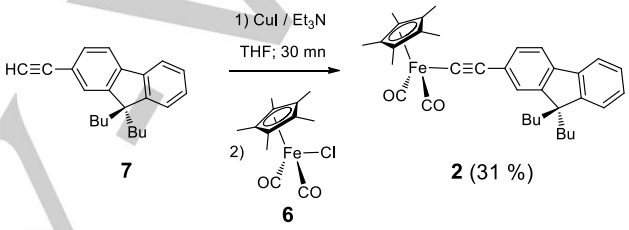

Scheme 3. Synthesis of the Fe(II) Complex **5**.

Complex **2** was characterized by mass spectrometry (ESI). Thus, a molecular peak corresponding to a cationic adduct with sodium, which forms during the ionization process, was detected, along with fragments corresponding to the successive loss of the two carbonyl ligands. The presence of the C_5Me_5 and of the 9,9-dibutyl-*9H*-fluorenyl fragments in the correct stoichiometry is evidenced by ^{1}H NMR and by ^{13}C NMR, while the two carbonyl ligands and the alkynyl bridge are revealed by diagnostic stretching modes in the IR spectrum (ν_{CO} at 2017 and 1967 cm^{-1}; $\nu_{C\equiv C}$ at 2093 cm^{-1} in dichloromethane) and also by characteristic peaks in the ^{13}C NMR spectrum of the complex (Experimental Part).[3g]

Synthesis and Characterization of the Ru(II) Complexes 3-4. The synthesis of the alkynyl complex **3** was effected from the Ru(II) chloride precursor **8** and the organic 2-alkynyl-9,9-dibutyl-*9H*-fluorene (**7**) previously reported,[11] following a classic workup (Scheme 4).[13] The vinylidene complex (**3-*v***) isolated by precipitation as an intermediate was not characterized, but readily deprotonated with triethylamine to give the yellow complex **3** in fair yields (61 %) after chromatographic separation. The two butyl groups at the 9-position of the fluorene group ensure a good solubility of this complex.

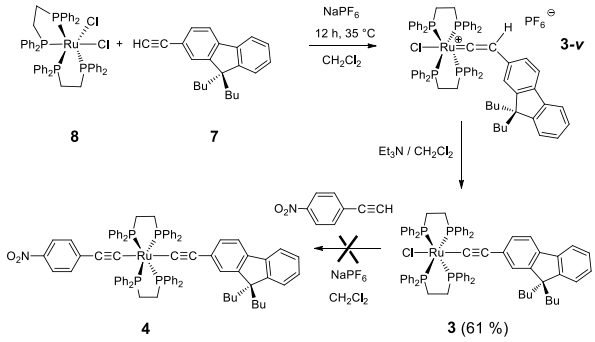

Scheme 4. Synthesis of the Ru(II) Complex **3**.

The red bis-acetylide complex **4** was obtained in fair yields from the known monoalkynyl complex **9** by substitution of the chloride with **7**, after deprotonation, in the presence of $NaPF_6$ and Et_3N in dichloromethane (Scheme 5).[14] In this case, the intermediate vinylidene complex was not isolated but rather was deprotonated *in situ* before the chromatographic purification. **4** could not be isolated pure by reacting **3** with ethynyl(4-nitrobenzene) following a similar reaction pathway (Scheme 4). In contrast, it has been reported that the synthesis of such dissymmetrical complexes are often more facile from the mono-acetylide precursor with the more electron-releasing arylalkynyl ligand.[3a,13b]

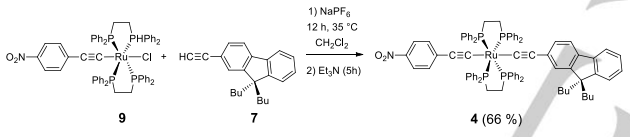

Scheme 5. Synthesis of the Ru(II) Complex **4**.

The two Ru(II) complexes **3** and **4** were characterized by mass spectrometry (ESI-MS), elemental analysis and by the usual spectroscopies.[13b,14b,15] The ^{31}P NMR singlets observed for **3** and **4** at 50.2 ppm and 53.2 ppm, respectively, are characteristic of these mono- and bis-alkynyl complexes.[13b] The presence of an additional fluorenyl group is readily established by ^{1}H NMR and ^{13}C NMR spectroscopies, when the spectra of **3** and **4** are compared to those of the starting complexes **8** and **9**, while the presence of the triple bond(s) is confirmed by observation of a strong $\nu_{C\equiv C}$ absorption in the infrared (IR) spectrum. This band is observed at 2066 cm^{-1} for **3** and at 2046 cm^{-1} for **4** in dichloromethane. Interestingly, only one band is observed for the latter complex, in spite of the presence of two alkynyl bonds. A closer examination of the infrared spectrum of **4** in KBr, however, reveals a broader absorption band with a shoulder at *ca.* 2070 cm^{-1}, suggesting that both vibrational modes certainly overlap, as previously observed in related bis-alkynyl Ru(II) complexes.[3a,14a,15a,16] The presence of the nitro group is confirmed by the appearance of diagnostic symmetric and asymmetric NO_2 stretches near 1580 cm^{-1} and 1324 cm^{-1}, respectively. Small red crystals of **4** were grown by slow evaporation of methanol-dichloromethane mixtures and the resulting X-ray structure definitively established the identity of this compound (Figure 1).

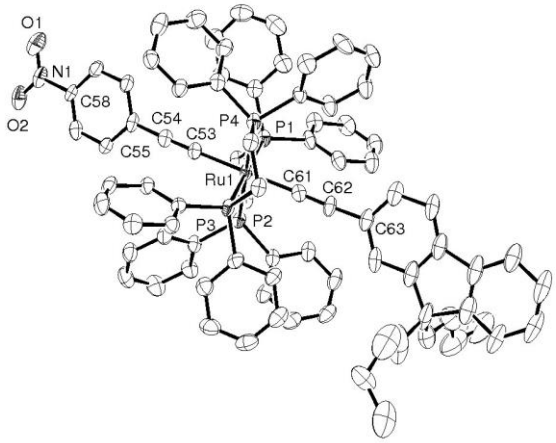

Figure 1. ORTEP representation of the dissymmetric complex **4** at the 50 % probability level. Selected distances (Å) and angles (deg): Ru1-P1 2.3717(17), Ru1-P2 2.3603(16), Ru1-P3 2.3740(16), Ru1-P4 2.3584(16), Ru-C53 2.039(6), Ru1-C61 2.062(6), C53-C54 1.229(8), C54-C55 1.435(8), C61-C62 1.219(8), C62-C63 1.422(8), C58-N1 1.459(7), N1-O1 1.234(7), N1-O2 1.216(7), P1-Ru1-P2 82.24(6), P3-Ru1-P4 81.63(6), P1-Ru1-C61 98.44(16), C53-Ru1-C61 179.3(2), P2-Ru1-C53 89.76(16), Ru1-C53-C54 176.0(5), C53-C54-C55 176.9(7), Ru1-C61-C62 175.8(5), C61-C62-C63 177.3(7), O1-N1-O2 123.3(6).

Solid-state Structure of 4. The complex **4** (Figure 1) crystallizes in the triclinic *P*-1 symmetry group, with one molecule of complex in the asymmetric unit and two dichloromethane molecules as solvates (see Experimental Section for details). The bond lengths and angles of this complex are not unusual in comparison to available X-ray data for related mononuclear bis-dppe Ru(II) bis-acetylide complexes and warrant no further comments.[3a,15a] As often stated for related complexes,[15a-c,17,18] the nitro group is coplanar with the nearby phenyl ring (torsion angle less than 0.04°), in line with a possible interaction between these fragments.[19] Also, the mean planes for the fluorenyl and phenyl ring are nearly coplanar exhibiting an angle of less than 2°, in a conformation allowing for optimal interaction of the π-manifold through the central ruthenium atom. These planes roughly bisect the two P-Ru-P' quadrants defined by the phosphorus atoms belonging to distinct dppe ligands, in line with a conformation minimizing any intramolecular steric congestion.[3a]

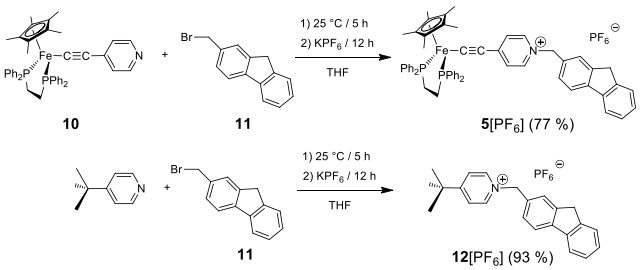

Scheme 6. Synthesis of the Fe(II) Complex **5**[PF_6].

Synthesis of the Fe(II) Pyridinium Complex 5[PF_6]. The complex **5**[PF_6], with an appended fluorenyl group, was obtained

from reaction of the known pyridine complex **10**[20] with 2-bromomethyl-*9H*-fluorene (**11**), following a reaction previously used to access the corresponding methylpyridinium complexes (Scheme 6).[21] This purple compound was isolated by selective precipitation in good yield (77 %) from the reaction medium and was characterized by elemental analysis, mass spectrometry ^{31}P, ^{1}H, and ^{13}C NMR and IR spectroscopies (Experimental Part). In the ^{1}H NMR spectrum, the bridging methylene-pyridinium protons appear as a singlet at 5.30 ppm, to low field of the two methylene protons at the 9 position of the fluorenyl group. Both the singlet observed at 98.1 ppm in the ^{31}P NMR spectrum and the $\nu_{C\equiv C}$ band observed at rather low-energy in the IR spectrum for a Fe(II) acetylide complex (1987 cm^{-1} in dichloromethane)[22] are typical signatures of such pyridinium alkynyl complexes.[21] In order to have an organic model of the alkynyl ligand of complex **5**[PF_6], we have also isolated the corresponding pyridinium salt **12**[PF_6] (Figure 6), which was fully characterized by the usual means as well as by X-ray crystallography (Figure 2 and ESI). This salt crystallizes in the monoclinic *P* 2_1/*n* symmetry group.

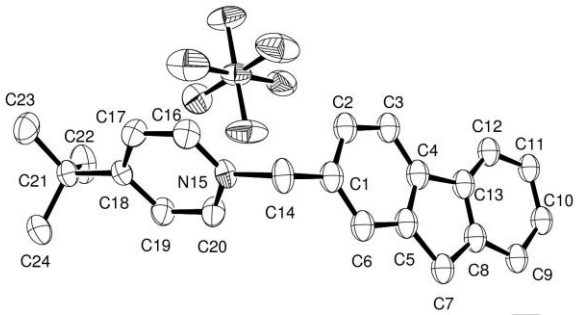

Figure 2. ORTEP representation of the pyridinium salt **12**[PF_6] (conformation A) at the 50 % probability level. Selected distances (Å) and angles (deg): C20-N15 1.340(3), C20-C19 1.370(3), C19-C18 1.387(3), C18-C17 1.385(3), C17-C16 1.374(3), C16-N15 1.332(3), N15-C14 1.502(3), C14-C1 1.511(8), N15-C14-C1 111.8(3).

Cyclic Voltammetry. Cyclic voltammograms were recorded for **2**-**5**[PF_6]. For the carbonyl complex **2**, a fully irreversible event can be observed near 0.9 V which certainly corresponds to metal-centred oxidation, while a fully irreversible reduction is observed at -1.40 V. Similar to **1**,[11] **3** and **4** exhibit pseudo-reversible metal-centered oxidations (Table 1). As expected from the literature, [3a,14a] relative to **1**,[23] this oxidation potential is significantly shifted to more positive values, the shift being more pronounced for the complex **4** due to the presence of the nitrophenylalkynyl ligand. The other redox event observed for this compound (at ca. -1.22 V) corresponds to the reduction of the nitro group.[14a] Finally, and unsurprisingly,[21] the potential of the metal-centered oxidation of the cationic pyridinium complex **5**[PF_6] is shifted toward positive values relative to **1**. The pyridinium-based reduction could not be observed, but was seen as an irreversible event at -1.37 V for the organic pyridinium derivative **12**[PF_6].

$$\Delta G_{CT} = E°(D^+/D) - E°(A/A^-) + (Z_A - Z_D - 1)e^2/4\pi\varepsilon_0\varepsilon d \qquad (1)$$

Based on the Rehm-Weller) equation (1),[24,25] these data were used to derive an estimate of the free enthalpy of formation of the intramolecular CS state (ΔG_{CS}) resulting from the oxidative quenching of the LC state (Scheme 2).[26] The latter is given by the difference between the metal-based oxidation potential and the first reduction potential of the fluorenyl group in CH_2Cl_2 (Table 1), corrected by an electrostatic term. Since the fluorene reduction peak cannot be observed in CH_2Cl_2, the reduction potential considered was that reported for fluorene in DMF (-2.9 V *vs.* SCE),[27] corrected for the change in the dielectric constant of the solvent (*ca.* -3.0 V in CH_2Cl_2). For the organic salt **12**[PF_6] which has no metal center, a ΔG_{CS} value resulting from electron transfer from the fluorene ligand to the pyridinium group was determined instead, based on the oxidation potential reported for fluorene in CH_2Cl_2 (1.48 V *vs.* SCE) and the reduction potential experimentally found for that salt.[27] In line with our expectations, we can see that significant changes in ΔG_{CS} take place between **1** and **3**, **4** and **5**[PF_6]. Note also that for both **4** and **5**[PF_6], two other CS states can be found at lower energy (denoted CS' and CS", respectively, in the following). Thus, for **4**, there is a state in which the fluorene ligand is oxidized and the 4-nitrophenyl moiety is reduced (CS') and a state in which the Ru(II) center is oxidized and the 4-nitrophenyl moiety is reduced (CS"), while for **5**[PF_6], there is a state in which the fluorene ligand is oxidized and the pyridinium moiety is reduced (CS') and a state in which the Fe(II) center is oxidized and the pyridinium moiety is reduced (CS"). Based on a reductive-trapping instead of an oxidative-trapping mechanism of the fluorenyl-based LC state, the CS' states offer a competitive deactivation pathway. Such a reductive quenching process is certainly operative in the compound **12**[PF_6] (see later). In contrast, the CS" states are not relevant for the quenching process under consideration, since they cannot be generated by a single electron transfer from the photogenerated CS state.

Table 1. Electrochemical Data for the 2-Fluorenyl Complexes **1-5**[PF_6] and for **12**[PF_6].

Cmpd	E^{0} [a]	ΔE_p [b]	i_c/i_a	ΔG_{CS} [c]	Ref.
7	-0.17	0.08	1	2.63	[11]
2	-1.41	/	NR	>3.70	this work
	0.90	/	NR		
3 [d]	0.41	0.07	1	3.21	this work
4 [d]	-1.22	0.11	1	3.30	this work
	0.50	0.07	1	2.61 [e]	
				1.54 [f]	
5[PF_6]	0.25	0.08	1	3.26	this work
				2.87 [g]	
				1.66 [h]	
12[PF_6]	-1.39	/	NR	2.87 [g]	this work

[a] All E° values are in V *vs.* SCE. Conditions (unless specified): CH_2Cl_2 solvent, 0.1 M [N*n*Bu_4][PF_6] supporting electrolyte, 25 °C, Pt electrode, sweep rate 0.1 V s^{-1}. Unless specified, the ferrocene complex was used as an internal reference for potential measurements. [b] Difference between cathodic and anodic peak potentials. [c] Computed (in eV) according to eq. 1 (see text). [d] The Fe(κ^2-dppe)(η^5-C_5Me_5)(C≡CPh) complex was used as an internal reference for potential measurements (E° = -0.15 *vs.* SCE).[28] [e] Computed considering the reduction of the nitrophenyl group by the fluorenyl group (see text). [f] Computed considering the reduction of the nitrophenyl group by the Ru(II) center (see text). [g] Computed considering the reduction of the pyridinium group by the fluorenyl group (see text). [h] Computed considering the reduction of the pyridinium group by the Fe(II) center (see text).

Table 2. UV-vis Absorption and Emission Data for Selected M(II) and M(III) Complexes in CH_2Cl_2.

Cmpd	Absorption:		Emission:			
	λ_{max} / nm (10^{-3} ε in M^{-1} cm^{-1})	λ_{max}[a] / eV	λ_{ex}[b] / nm / eV	λ_{em}[c] / nm / eV	$\Phi_{\lambda lum}$ [d]	Ref.
1	278 (sh, 33.4), 296 (sh, 30.0), 404 (20.0)	3.07	291 / 4.26	334 / 3.71	0.4 %	[11]
2 [e]	338 (30.6) [f]	3.67	/	/	/	This work
3	251(37.6), 286 (sh, 15.9), 352 (sh, 22.2), 373 (24.9)	3.32	290 / 4.28	331 / 3.74	0.8 %	This work
4	275 (sh, 59.8), 367(29.8), 489 (18.3)	2.53	290 / 4.28	319 / 3.89	1 %	This work
5[PF_6]	266 (49.8), 304(27.6), 322 (sh, 18.7), 540 (sh, 18.1), 586 (21.1)	2.12	285 / 4.35	NL [g]	/	This work
3[PF_6] [h]	276 (38.2), 309 (sh, 18.3), 439 (16.8), 454 (sh, 12.7), 640 (3.5), 902 (14.5)	1.37	/	/	/	This work
4[PF_6] [h,i]	269 (47.1), 317 (26.2), 440 (27.0), 451(sh, 23.9), 680 (0.5), 992 (sh, 11.0),1155 (16.9)	1.07	/	/	/	This work
12[PF_6]	266 (31.3), 304 (14.1)	4.08	265 / 4.68	320 / 3.87 520 / 2.38	2 % 1 %	This work
13	282 (13.7), 376 (sh, 1.0)		/	/	/	This work
14[PF_6]	266 (sh, 18.4), 316 (13.1), 546 (sh, 17.9), 578 (19.6)		/	/	/	[21, 36]

[a] Lowest absorption maximum. [b] Excitation wavelength. [c] Emission wavelength. [d] Luminescence yield. [e] Photosensitive product which decomposes during the measurement. [f] Vibronically structured peak. [g] No luminescence detected. [h] Values obtained by spectroelectrochemistry in the presence of 0.2 M [Bu_4N][PF_6]. [i] Spectroelectrochemistry run at 243 K (see text).

Linear Optical Properties of the M(II) Complexes. The UV-Vis/near-IR absorption spectra of **2-4** and **5**[PF_6] were next recorded in dichloromethane (Table 2 and Figure 3).

Absorption Spectroscopy. The spectrum of the Fe(II) carbonyl complex **2** is quite simple, consisting mostly of an absorption band at 338 nm (3.67 eV). This absorption likely corresponds to the $(\pi^*)_{Flu} \leftarrow d_{Fe}$ MLCT band, since its energy matches fairly well with the energy (ΔG_{CS}) of the corresponding CS state at 3.70 eV (Table 1).[29] The shoulders on the high energy side of this absorption band could result from an unresolved vibronic structure or from overlap with other absorptions. The intensity of this band is higher than that of the corresponding MLCT band of **13** (Scheme 7), the known analogue of **2**,[29-30] suggesting that this band certainly overlaps with another weaker band which might correspond to a fluorene-based LC band. However, further studies with this complex were not attempted, since this compound was photosensitive and decomposed in the UV cell under irradiation or even in daylight. This unexpected instability is possibly related to the well-known photolability of the CO ligand in these piano-stool compounds.[31]

For the Ru(II) complexes, the lowest energy absorptions at 373 nm for **3** and at 489 and 367 nm for **4** correspond to transitions with a strong metal-to-ligand charge transfer (MLCT) character ($\pi^* \leftarrow d_{Ru}$), as indicated by DFT calculations (see later). The MLCT transition at lowest energy for **4** is at the origin of the deep red color of this compound. It corresponds to a MLCT transition toward the nitrophenyl group which is the most electron deficient alkynyl ligand of this complex and usually gives rise to transitions in this energy range.[15a-c,32,33] The second MLCT absorption of this complex resembles that observed for **3** and corresponds to a charge transfer directed toward the 2-ethynylfluorenyl ligand. We note again a fairly good match with the energy of the corresponding CS states (ΔG_{CS}) derived from electrochemical data (compare Table 1 and Table 2). Finally, the next-higher-energy transitions of **3** and **4** are attributed to a set of overlapped transitions including the fluorenyl-based ($\pi^* \leftarrow \pi$) LC charge transfer transition. The latter corresponds possibly to the shoulder on the high energy side of this huge absorption band, near 300 nm, as has already been seen for the iron derivative **1**.[11]

Scheme 7. Organoiron Alkynyl Complexes Related to **2** and **5**[PF_6].

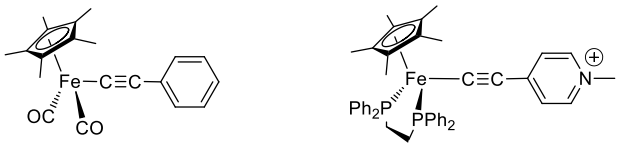

13 **14**[PF_6]

Finally, the cationic pyridinium Fe(II) complex **5**[PF_6] presents electronic transitions at significantly lower energies. While no calculations have been conducted on that complex, this transition at lowest energy must also correspond to an MLCT transition from the metal center toward the pyridinium moiety ($\pi^*_{Py} \leftarrow d_{Fe}$), as indicated by the good match with the energy (ΔG_{CS}) of the corresponding CS state (compare Table 1 and Table 2).[34] The next-higher-energy (and sizeable) absorption band, which appears as a huge and composite band in the far UV range, peaks at 266 nm. It certainly overlaps with the fluorene LC band, which could correspond to the shoulder on this band observed on its low energy side. In accordance with such an hypothesis, a shoulder of similar intensity was not observed with the methylpyridinium analogue **14**[PF_6] (Scheme 7) of **5**[PF_6].[35]

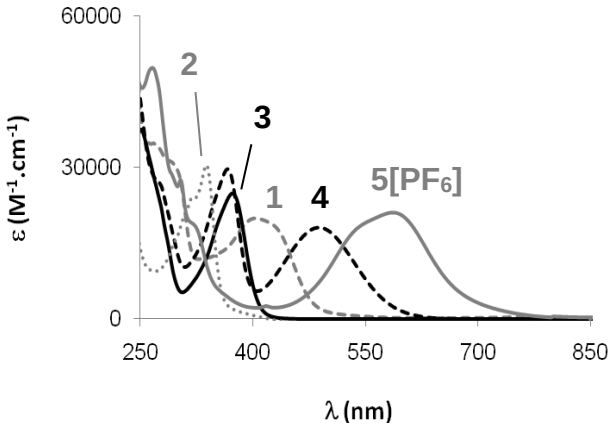

Figure 3. UV-Vis Spectra for Complexes **1** and **2-4, 5**[PF_6] in CH_2Cl_2 at 25 °C.

Emission Spectroscopy. No attempts were made to detect fluorescence for complex **2** due to its aforementioned photochemical instability. However, upon excitation in the 285-295 nm range, the Ru(II) complexes **3** and **4** were luminescent. The yields found for **3-4** in CH_2Cl_2 solutions are roughly twice that previously found for the Fe(II) complex **1** (Figure 4),[11] with an emission maximum located slightly to the blue of that of **1**. Their fluorescence yields are significantly lower than that of 9,9-dibutyl-4-ethynylfluorene (**7**) (Φ_{lum} = 58%)[11] and also significantly lower than that reported for fluorene in cyclohexane (Φ_{lum} = 72%).[37]

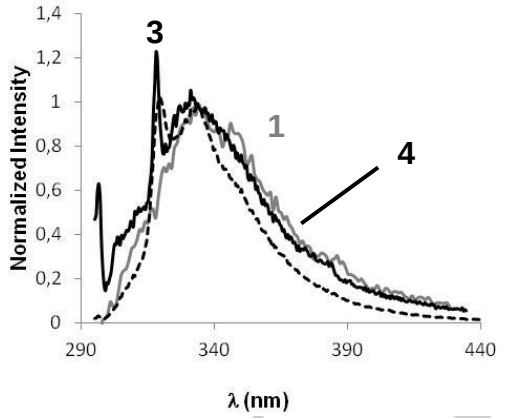

Figure 4. UV-Vis emission spectra for complexes **1** and **3-4** in CH_2Cl_2 at 25 °C.

Under similar conditions, no luminescence could be detected for **5**[PF_6], while that of the organic pyridinium salt **12**[PF_6] was much lower than that of **7**.[38] Based on the electrochemical data (Table 1), intramolecular oxidative quenching of the LC state in **12**[PF_6] by the pyridinium is possibly taking place and contributing to the weak luminescence yield, the remote fluorene-group this time playing the role of reductant. Pyridinium derivatives are often poor fluorophores[39] because their relatively low reduction potential makes them efficient luminescence quenchers.[40]

Linear Optical Properties of the Ru(III) Complexes. The Ru(III) complexes **3-4**[PF_6] were generated from their Ru(II) parents by spectroelectrochemistry in an OTTLE cell and their electronic spectra were recorded (Table 2, Figure 5 and ESI). In contrast to **3**[PF_6] for which the original spectrum could be restored upon back-reduction to the starting complex **3**, the oxidation of **4** was only chemically partially reversible at 25 °C and had to be performed at lower temperature (-30 °C) to become fully reversible in the chemical sense. The spectrum of these complexes is typical of Ru(III) bis-alkynyl complexes,[41] and reveals that oxidation switches on an intense absorption with a strong LMCT character in the near-IR range for both compounds. According to calculations made on related complexes,[14a,41] the next (higher) transitions are often multiconfigurational and should be described as $\pi^* \leftarrow \pi$ transitions involving aryl alkynyl carbon and metal MOs.

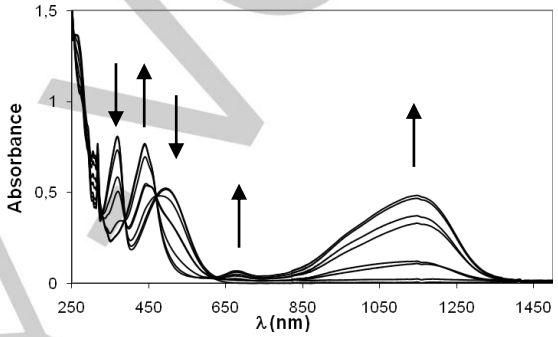

Figure 5. Spectroelectrochemistry in the near UV-Vis-near-IR range for Complex **4** in CH_2Cl_2 (0.2 M TBAH) at -30 °C.

Nonlinear Optical Properties. We next determined the cubic hyperpolarizabilities of **3** and **4** by Z-scan, using femtosecond laser pulses at various incident wavelengths between 550/600 and 1600 nm in CH_2Cl_2 solutions (Figure 6, Table 3). These compounds have TPA maxima coinciding approximately with twice the UV-Visible λ_{max} values (Table 2), indicating that the allowed excited states at lowest energy give rise to two-photon absorption. Thus, the first MLCT state of **4** has an apparent TPA cross-section twice stronger than that of compound **3**. This is because these transitions correspond to different charge transfers; that in **4** is directed from the metal toward the nitroaryl group, whereas that in **3** is directed toward the fluorenyl group ($\pi^*_{PhNO2} \leftarrow \pi_{C\equiv CPh}/d_{Ru}$), as demonstrated by DFT calculations (see later). The second MLCT band of **4** at 367 nm corresponds to the first MLCT band of **3** ($\pi^*_{Flu} \leftarrow \pi_{C\equiv CFluo}/d_{Ru}$). When these are compared, we see that upon progressing from **3** to **4**, the replacement of the chloride by the nitrophenylalkynyl ligand causes a four-fold increase in the apparent TPA cross-section near 700 nm. The strong linear absorptivity between 500 and 600 nm gives a saturable absorption (SA) effect at these wavelengths which complicates the determination of apparent TPA for **4** in this spectral range, resulting in larger experimental errors for this second TPA maximum.

Table 3. Nonlinear Optical Data at Wavelengths of Apparent 2PA Extrema for **1**, **2-4** and **15** in CH_2Cl_2 (unless otherwise indicated).

	λ_{TPA} (nm)	γ_{re} (10^{-34} esu)	γ_{im} (10^{-34} esu)	$\lvert\gamma\rvert$ (10^{-34} esu)	σ_2 (GM)	Ref
1	740	-160 ± 17	84 ± 16	180 ± 25	2400 ± 470	[11]
1[a,b]	740	-25 ± 15	14 ± 2	28 ± 15	330 ± 50	[11]
3	720	-15 ± 5	12 ± 2	19 ± 5	360 ± 60	This work
4	700	-490 ± 55	51 ± 7	490 ± 55	1600 ± 230	This work
	1000	-35 ± 70	55 ± 19	65 ± 73	860 ± 290	This work
15	700	-85 ± 10	31 ± 5	90 ± 11	1700 ± 30	[11]
	760	-87 ± 9	14 ± 2	88 ± 9	370 ± 60	[11]

[a] Determined in THF. [b] Data obtained at Wroclaw University of Technology. All other data were obtained at the Australian National University.

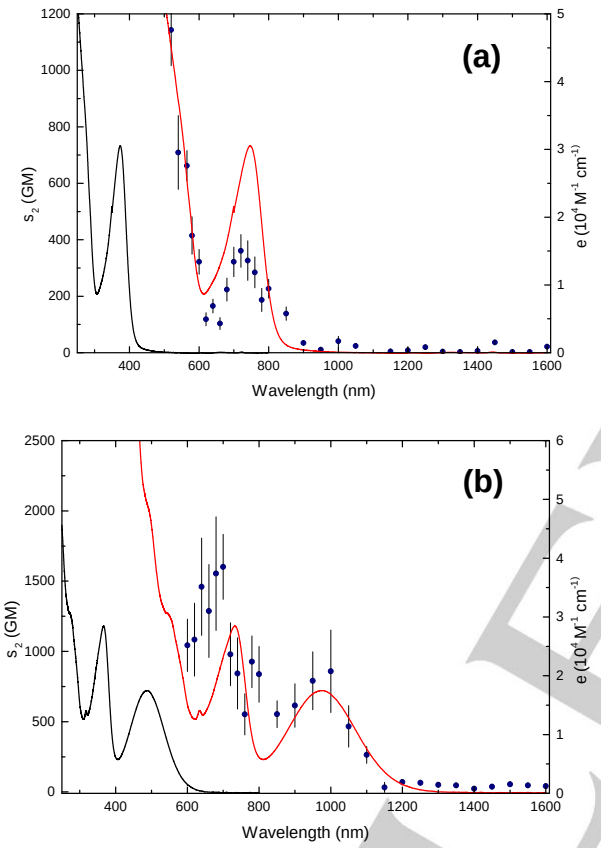

Figure 6. Cubic hyperpolarizabilities determined for **3** (a) and **4** (b) in CH_2Cl_2 at 25 °C by open and closed-aperture Z-scan measurements.

DFT Calculations. Calculations on C_s-symmetric models **3-Me** and **4-Me** have been performed. These differ from **3-4** by replacement of the dppe ligands by dmpm (bis(dimethyl-phosphino)methane) and the *n*-butyl groups on the fluorenyl unit by methyl groups. After structural optimization (ESI), the calculations reveal that the frontier molecular orbitals (FMO) of the mono-alkynyl derivative **3-Me** consist of a HOMO mostly localized on the ruthenium alkynyl fragment and a LUMO localized on the fluorenylalkynyl fragment. For the bis-alkynyl derivative **4-Me**, the HOMO is now localized on the ruthenium bis-alkynyl fragment and the LUMO is localized on the nitrophenyl fragment, resulting in a significant reduction in the HOMO-LUMO (*ca.* 1.7 eV) in **4-Me** compared to **3-Me** (Figure 8). The assignment of the first oxidation step as metal-localized for these complexes is therefore mostly formal[42] and perhaps less accurate than in the case of the Fe(II) complex **1** previously studied.[11]

TD-DFT calculations were then performed on the Ru(II) complexes in order to gain some insight into the nature of the allowed low-energy transitions in the visible range (Table 4). As previously observed for **1**, the energies of the various allowed transitions are underestimated by *ca.* 2000-3000 cm^{-1}. This is attributable to some extent to the neglect of solvent and structural simplifications brought on the compounds. Nevertheless, some useful qualitative information can be obtained on the nature and energy ordering of the main allowed singlet-singlet transitions. Thus, the first strongly allowed transition found for **3-Me** corresponds to the LUMO ← HOMO transition with a dominant MLCT character ($\pi^*_{Fluorene} \leftarrow d_{Ru}+\pi_{C\equiv C}$). For **4-Me**, the same picture holds except that the MLCT transition at lowest energy corresponds now to charge transfer transitions towards the nitrophenyl ring rather than toward the fluorenyl fragment ($\pi^*_{C6H4NO2} \leftarrow d_{Ru}$), while the next-higher-energy allowed transitions correspond to a set of MLCT transitions toward the fluorenyl fragment (Figure 9). While the former transition corresponds formally to population of the CS" state at lowest energy (Table 1), the second one corresponds to that at higher energy for that particular compound (CS). Note however that a long range ligand-ligand charge transfer (LLCT) transition from the fluorene to the nitrophenyl ($\pi^*_{C6H4NO2} \leftarrow \pi_{Fluorene}$) that would formally give rise to the intermediate CS' state was not found among the allowed transitions. Finally, for both compounds, transitions with more pronounced LC character on the fluorene are found at higher energy. In contrast to the corresponding transition in **1**, which was nearly free of any metal character, our calculations indicate that some metal character is still present in these, as might have been expected given the more pronounced d/p mixing usually observed with Ru(II) alkynyl complexes compared to their isoelectronic Fe(II) counterparts.

Table 4. Observed and Calculated Optical Transitions for **3-Me** and **4-Me**.

Cmpd	ν_{max}[a] [ε][b] (Exp)	ν_{max}[a] [f][c] (Calc)	Composition (Weight %)	Major Assignment
3-Me	26810 [0.25]	23832 [0.13]	57a'' → 58a'' (87%)	Ru_{dyz} (24%) + π_{Cl} + π_{C2Fluo} → π^*_{C2Fluo}
	28409 [sh, 0.18]	27948 [0.04]	56a'' → 58a'' (85%)	Ru_{dyz} (12%) + p_{pz} + π_{Cl} → π^*_{C2Fluo}
	39841 [0.38]	33410 [0.09]	55a'' → 58a'' (58%)	Ru_{dyz} (6%) + p_{Pz} + π_{C2Fluo} → π^*_{C2Fluo}
4-Me	20450 [0.18]	15968 [0.05]	125a' → 126a' (70%)	Ru_{dxy} (30%) + π_{C2C6H4} + πC2 → $\pi^*_{C2C6H4NO2}$
		20056 [0.11]	124a' → 126a' (65%)	π_{C2Ph} + π_{C2} + p_y → $\pi^*_{C2C6H4NO2}$
	27248 [0.30]	23269 [0.10]	66a'' → 67a'' (85%)	Ru_{dxz} (30%) + π_{C2} + $\pi_{C2PhFluo}$ → π^*_{C2Fluo}
		28856 [0.11]	65a'' → 67a'' (78%)	Ru_{dxz} (14%) + p_y + π_{C2} + $\pi_{C2C6H4Fluo}$ → π^*_{C2Fluo}
	36364 [0.27]	30502 [0.03]	121a' → 126a' (79%)	Ru_{dxz} (35%) + π_{C2} + π_{C6H4} → $\pi^*_{C2C6H4NO2}$
		33813 [0.07]	66a'' → 73a'' (48%)	Ru_{dxz} (30%) + π_{C2} + $\pi_{C2C6H4Fluo}$ → $\pi^*_{C2C6H4Fluo}$
			64a'' → 67a'' (40%)	p_y + π_{C2} + $\pi_{C2C6H4Fluo}$ → $\pi^*_{C2C6H4Fluo}$

[a] Calculated (for **3-Me** and **4-Me**) and observed (for **3**-**4**) ν_{max} in cm^{-1}. [b] Extinction coefficient in 10^5 M^{-1} cm^{-1}. [c] Calculated oscillator strength [*f*].

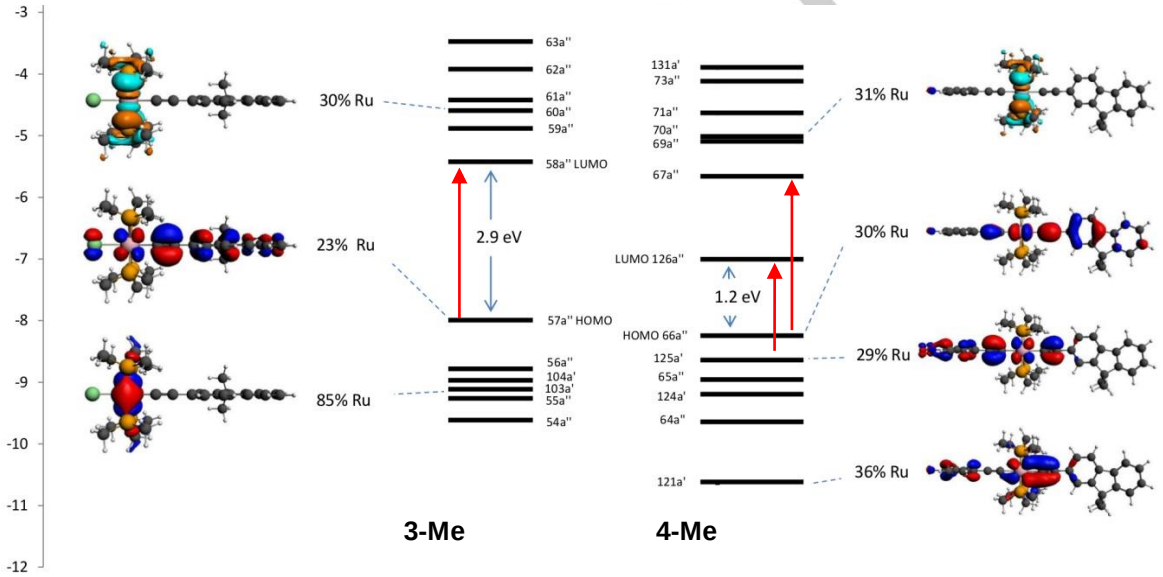

Figure 8. Frontier molecular orbitals for **3-Me** and **4-Me** illustrating the first allowed calculated singlet-singlet transitions (red arrows). The metal-centred MOs are also shown.

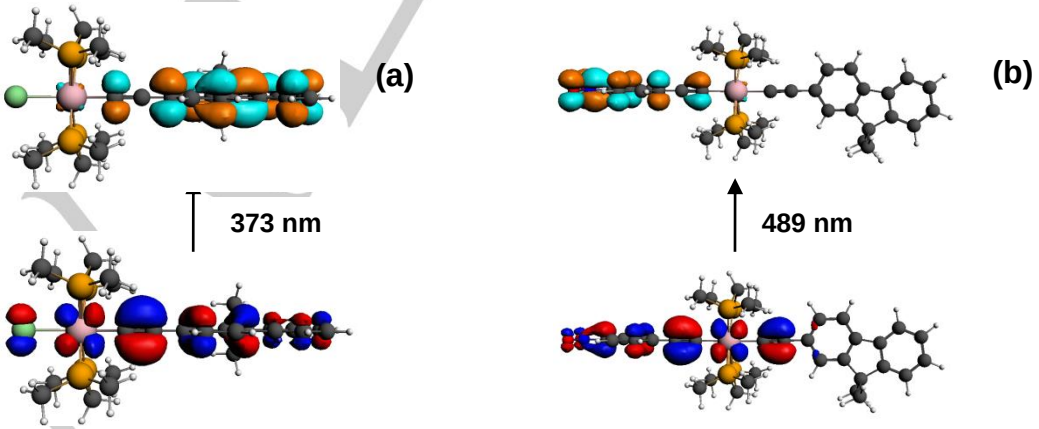

Figure 9. Plots of the frontier molecular orbitals for **3-Me** (a) and **4-Me** (b) predominantly involved in the first allowed transition. Contour values are ± 0.03 $(e/bohr^3)^{1/2}$.

Discussion

The targeted compounds **2**-**4** and **5**[PF_6] could be isolated and characterized. While **2** turned out to be photosensitive in solution, fluorimetric studies on **3** and **4** revealed a marginally higher luminescence than for **1**, whereas (**5**[PF_6]) was not emissive at all in solution. The luminescence of **3** and **4** is too weak to measure their TPA cross-sections by two-photon excited fluorescence (TPEF). In line with previous investigations conducted on **1** and **15** (Scheme 8),[11] we find that the luminescence of **3** and **4** does not originate from their lowest MLCT excited state, which turns out to be essentially non-emissive in solution at 25 °C, but rather from an excited state higher in energy. Although such an emissive behavior is rare,[43] we note that related observations have been independently reported for other alkynyl complexes such as **16a-c** or **17** (Scheme 8).[8e, 44] Such unusual behaviour could be induced by the electronic decoupling of the fluorenyl fragment from the rest of the molecule,[44] a situation perhaps achieved for selected rotamers of **1**, **3** and **4** in solution.

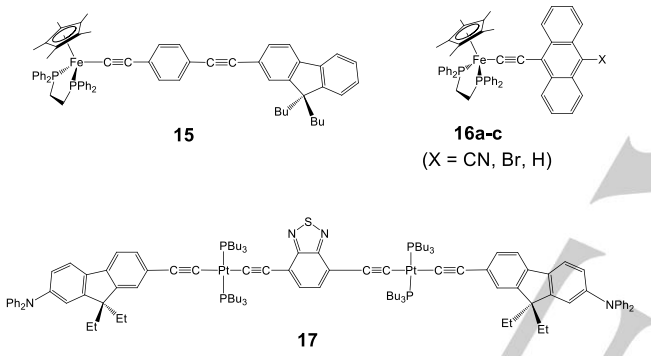

Scheme 8. Related Organoiron Complexes Showing Dual Fluorescence.

Marcus Analysis of a Hypothetical Redox-Based Luminescence-Quenching Process. Considering that, as proposed in Scheme 2, the weak quantum yields of **1**, **3** and **4** originate from an intramolecular redox-quenching reaction, we have tried to learn more about this particular process. To this aim, the effect of a change in metal-centred oxidation potential on the luminescence quantum yields was closely examined for these compounds. As already mentioned above, when the latter are compared to that of 2-ethynylfluorene (**7**), the presence of the organometallic Ru(II) center in **3** or **4** appears to result in a luminescence quenching nearly as efficient as that induced by the presence of the Fe(II) center in **1**. Based on eq. 1 and assuming that the radiative rate (k_{lum}) remains constant between **1**, **3** and **4** (a likely assumption considering that the LC state is fluorene-based),[46] this means that the global non-radiative decay rate (k_{eT} + k_{NR}) has roughly been halved for **3** and **4**. In comparison, the absence of fluorescence for **5**[PF_6] is less informative since the weak luminescence found for **12**[PF_6] indicates that the non-radiative decay is already quite efficient in the pyridinium moiety. Unsurprisingly, the presence of the metal center in **5**[PF_6], by opening additional non-radiative deactivation pathways, renders this compound totally non-emissive.

Focusing on **1**, **3** and **4**, we see that estimates of the ΔG_{CS} values (Table 1) match fairly well with the energies of one of the MLCT [$(\pi^*)_{Flu}\leftarrow d_M$] states of these compounds (Table 2), considering that the latter correspond to "vertical" energies and therefore represent higher bounds of these values (Figure 10).[47] This indicates that these particular MLCT states will mediate the electron-transfer process underlying the non-radiative decay. After estimating the energy of the LC state (λ_{00}) from the absorption and emission curves obtained for **3** and **4** (see ESI), the thermodynamic driving forces (ΔG_{eT}) for the reductive electron-transfer trapping process can be obtained. These are always negative (-0.86 eV and -0.83 eV *vs.* -1.29 eV for **1**), in line with an exergonic process. For **4**, because of the presence of the easily reducible 4-nitrophenyl group in this complex, an oxidative quenching process of the LC state is also possible via the CS' state (Figure 10). The specific thermodynamic driving force ($\Delta G_{eT'}$) of this second process has been determined. It is even more exergonic (-1.52 eV) than the former ΔG_{eT}.

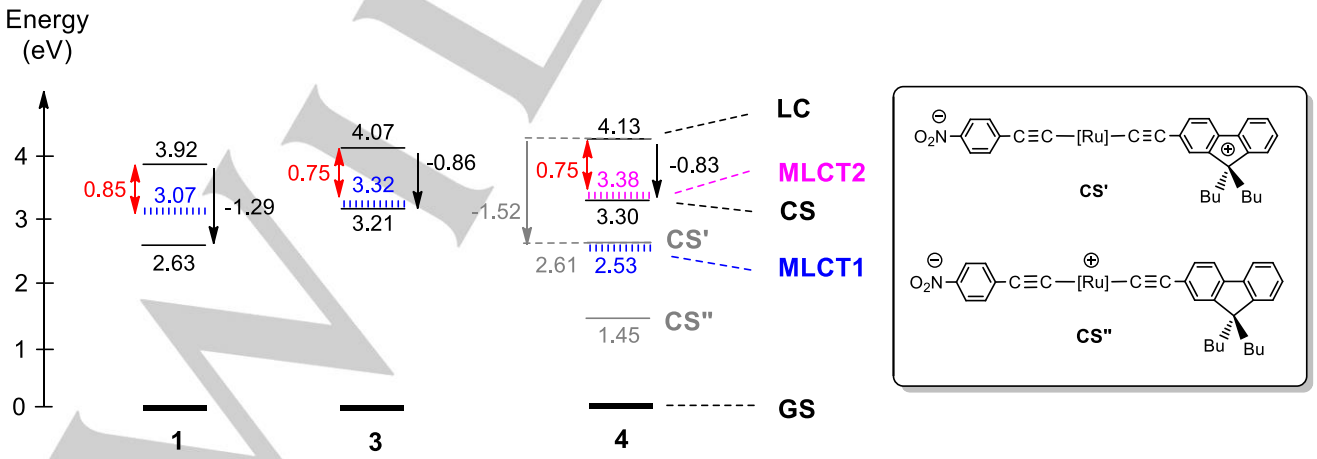

Figure 10. Comparative energetic ordering of the ground (GS) and fluorene-centred excited states (LC) for **1**, **3** and **4**. The two additional CS states CS' and CS" of **4** (in grey) are drawn in the inset ([Ru] = Ru(κ^2-dppe)$_2$). Vertical energies of the MLCT state(s) are given in blue (and purple). These energies were derived from the absorption maxima and should be considered as higher bound values. Energy differences (in eV) between the LC and the vertical energy of the closest MLCT state are given (in red) as well as ΔG_{eT} values (in black or grey).

According to Marcus,[12b] the electron transfer rate (k_{eT}) of the quenching process is determined mostly by its activation energy ($\Delta G^{\neq}$), given that the electronic coupling (H_{ab}) between the metal center and the fluorene chromophore should not vary dramatically within this series of compounds (eq. 3).[3g,48,49] Thus, $\Delta G^{\neq}$ values are essentially determined by ΔG_{eT} values and by the mean reorganization energies (λ) of the redox process (eq. 4). When sensible values are considered for λ, such as 0.6 ± 0.1 eV for **1**[50] and 0.9 ± 0.1 eV for **3** and **4**,[32] $\Delta G^{\neq}$ values of 0.0730 eV, 0.0005 eV and 0.0010 eV, respectively, can be derived. Also, a $\Delta G^{\neq}$ value of 0.0787 eV can be derived for the second and trapping mechanism (via the CS' state) in **4**.[51] This analysis indicates that, contrary to our initial belief, the most exergonic electron-transfer processes, corresponding also to complexes with the largest $M^{II/III}$ oxidation potentials, should be the slowest ones.

$$k_{eT} = C(H_{ab})^2 \exp(\Delta G^{\neq}/k_bT) \quad (3)$$

$$\Delta G^{\neq} = (\Delta G_{eT} + \lambda)^2/(4\lambda) \quad (4)$$

Based on these data, several statements can be made: (i) For **4**, and in spite of its larger exergonicity, the oxidative quenching mechanism of the LC state (via the CS' state) will not be competitive with the reductive quenching (via the CS state) initially proposed (Scheme 2). (ii) The redox quenching process proposed should be significantly faster for the Ru(II) complexes **3** and **4** than for the Fe(II) derivative **1**, at odds with what is suggested by the quantum yields measured for these compounds. (iii) Given that the $\Delta G^{\neq}$ values span nearly two orders of magnitude, the differences between the corresponding k_{eT} rates should be much larger. As a result, based on eq. 1, much more pronounced differences should have been observed between the fluorescence quantum yields (eq. 1) of **1**, **3** and **4** if k_{eT} was controlling the non-radiative relaxation and k_{lum} was remaining fairly constant. *In fine*, this analysis suggests that reductive electron-transfer *does not* constitute the dominant non-radiative relaxation process of the presumed luminescent LC state - another mechanism different from the photoinduced electron-transfer hypothesized in Scheme 2, such as internal conversion for instance,[52] must also play a determining role in the luminescence quenching process. Improvement of the luminescence yield of such complexes, if possible, will therefore require more than just fine-tuning their metal-based oxidation potential.

Third-Order NLO Activity of 3 and 4. In Table 3, the results are compared to those of **1** and **15** (Scheme 8) previously obtained under similar conditions. As often observed in the literature,[7e] the bis-acetylide derivative (**4**) which possesses an extended and more polarized π-manifold, appears to be significantly more active than **1** and **3** at 700 nm. This is apparently due to the larger refractive properties (γ_{re}) of these compounds which dominate their third-order NLO response over the wavelength range probed (ESI).

$$\gamma \propto -\mu_{ge}^4/E_{ge}^3 + \mu_{ge}^2\mu_{ee'}^2/E_{ge}^2E_{ge'} + \mu_{ge}^2(\mu_{ee} - \mu_{gg})^2/E_{ge}^3 \quad (5)$$

Based on the perturbation expression often used to express γ (eq 5),[7a, 54] the ordering found (**4** > **1** > **3**) can be inversely related to the HOMO-LUMO gaps of these complexes (Figure 8), which also determines the energy of the first allowed transition(s). Thus, **3** appears less NLO-active than **1** (and **15**), possibly consistent with its larger gap mostly induced by the larger electronegativity of Ru(II) over Fe(II).[11] In contrast, due to the presence of the low-lying LUMO centered on the nitro group which narrows the HOMO-LUMO gap, **4** exhibits the strongest NLO activity at 700 nm, and is even more active than **15**. Thus replacement of the chloride ligand by the 4-nitrophenylethynyl ligand upon progressing from **3** to **4** significantly improves the third-order NLO activity, in spite of the concomitant increase of the metal-centered oxidation potential.

Likewise, the TPA associated with the first MLCT band of **4** is significantly larger than that associated with the first MLCT band of **3**. As previously discussed, the first MLCT states are different in each compound and strongly polarized transitions such as that of **4** have already been shown to give rise to stronger two-photon absorption (TPA) than less polarized ones.[55] A closer look at the data reveals that the apparent TPA value associated with the first MLCT excited state of **3** ($\pi^*_{Fluorene} \leftarrow d_{Ru}+\pi_{C\equiv C}$) is clearly lower than that reported for **1** in CH_2Cl_2, although this corresponds to a similar MLCT.[11] Taken at face value, these data would indicate that Fe(II) is superior to Ru(II) for this particular property when ligated with a 2-ethynylfluorenyl ligand. However, the photochemical changes in CH_2Cl_2 previously noted for **1** during Z-scan measurements might perhaps have led to some overestimation of the measured TPA values in that particular solvent. In that respect, TPA values comparable to those of **15** were found for **1** when measured in THF (Table 3). Comparison of the second TPA peaks of **4** and **15**, which possess comparable metal-to-fluorene ($\pi^*_{Flu}\leftarrow d_M$) charge transfer character (M = Fe(II) and Ru(II)) exhibit nearly similar cross-sections. Interpretation of the changes in absolute values of these TPA cross sections between Fe(II) and Ru(II) must therefore be made with caution until more data are available.

Finally, spectroelectrochemical investigations conducted on **3**-**4** (Figure 3 and ESI) revealed that oxidation gives rise (reversibly) to a Ru(III) parent with an inverted polarization of the metal-alkynyl-fluorene π-manifold. As a result, an intense and broad LMCT band appears in the 850-1050 nm range while the MLCT band observed at lowest energy for the Ru(II) precursor disappears. While TPA (associated with a positive sign of γ_{Im}) takes place in this spectral range for the Ru(II) complex, SA (associated with a negative sign of γ_{Im}) is now observed for the Ru(III) isomer (Table 3). As previously shown for related mono- and bis- Ru(II) alkynyl complexes,[41] the LMCT states usually give rise to SA when excited. Thus, likewise to what had been previously stated for the redox-active analogues **1** and **15**,[11] oxidation of **3**-**4** leads to a "switch" of the sign of the imaginary part of the cubic NLO coefficient (γ_{Im}) near 900 nm,[56] itself associated with a dramatic change of the nonlinear absorption properties in this spectral range.[7a]

Conclusions

We have reported in this contribution the synthesis and characterization of four new Ru(II) and Fe(II) alkynyl complexes (**2-4** and **5**[PF_6]) containing 2-fluorenyl groups. Spectrochemical investigations reveal that the lowest lying (MLCT) singlet excited states of these compounds is essentially non-emissive. In line

with previous investigations on the related organoiron analogue **1**, the weak luminescence that can be detected for **3-4**, when excited around 300 nm, possibly originates from a higher lying excited state presumably centered on the fluorenyl group. As such, the luminescence quantum yields of these compounds remain too weak to allow the determination of their TPA cross-sections by two-photon induced fluorescence (TPEF). Finally, we show that both **3** and **4** exhibit significant third-order NLO responses in the near-IR range. Similar to **1**, the related (air-sensitive) mononuclear organoiron complex previously studied, these air-stable compounds behave as two-photon absorbers in the 850-1050 nm region, **4** being significantly more active than **1** and **3**. Furthermore, in this particular spectral range, these complexes should also give rise to a dramatic change in their NLO response upon oxidation, an observation emphasizing their interest for innovative developments based on the redox-switching of their third-order NLO properties.

Experimental Section

General. All manipulations were carried out under an inert argon atmosphere. Solvents and reagents were used as follows: MeOH, distilled from Mg/I_2; THF, Et_2O and *n*-pentane, distilled from Na/benzophenone; CH_2Cl_2, distilled from CaH_2 and purged with Ar, opened/stored under Ar. High-field NMR spectroscopy experiments were performed on multinuclear Bruker 500 MHz, 300 MHz or 200 MHz instruments (AVANCE 500, AM300WB and 200DPX). Chemical shifts are given in parts per million relative to tetramethylsilane (TMS) for ^1H and ^{13}C NMR spectra and external H_3PO_4 for ^{31}P NMR spectra. Transmittance-FTIR spectra were recorded using a Bruker IFS28 spectrometer (400-4000 cm^{-1}). UV-Visible spectra were recorded using a Cary 5000 spectrometer. Fluorescence spectra were recorded using an Edinburgh Instrument FLS 920 fluorimeter equipped with a 450 W Xenon lamp and a Peltier-cooled Hamamatsu R928P photomultiplier tube in photon-counting mode. MS analyses were performed at the "Centre Regional de Mesures Physiques de l'Ouest" (CRMPO, University of Rennes) on a high resolution MS/MS ZABSpec TOF Micromass Spectrometer. Elemental analyses were performed at the "Centre Regional de Mesures Physiques de l'Ouest" (C.R.M.P.O., University of Rennes). The solid-state structures (X-ray) were resolved at the "Centre de Diffractométrie X" (UMR CNRS 6226, University of Rennes).

Unless specified, all reagents were of commercial grade. Petroleum spirit refer to the 40-60 °C boiling range fraction. *cis*-Ru(κ^2-dppe)$_2$Cl$_2$ (**8**),[13a] *trans*-Ru(κ^2-dppe)$_2$[C≡C(4-$C_6H_4NO_2$)](Cl) (**9**),[15a] Fe(η^5-C_5Me_5)(CO)$_2$(Cl) (**6**),[57] Fe(η^5-C_5Me_5)(κ^2-dppe)[C≡C(4-C_5H_4N)] (**10**)[20], 2-alkynyl-9,9-dibutyl-9*H*-fluorene (**7**)[11] and 2-bromometyl-9*H*-fluorene (**11**)[58] were prepared analogously to published procedures.

Synthesis of compound 1: A solution of the fluorene derivative **4** (61 mg, 0.11 mmol) and TCNE (14 mg, 0.11 mmol) in CH_2Cl_2 (1.1 mL) was stirred at 20 °C for 15 h. The reaction mixture was concentrated under reduced pressure to give the title compound (75 mg, 100%) as a dark red solid. **MP**: 108-111 °C. ***R*$_f$**: 0.24 [Petroleum ether/Et_2O (9:1)]. **^{1}H NMR** (400 MHz, $CDCl_3$) δ = 7.83 (1H, d, *J* = 1.5 Hz, H_{Flu}), 7.72 (1H, d, *J* = 8.1 Hz, H_{Flu}), 7.71-7.67 (1H, m, H_{Flu}), 7.61 (2H, d, *J* = 9.3 Hz, H_{Ar}), 7.46 (1H, dd, *J* = 1.9 and 8.1 Hz, H_{Flu}), 7.39-7.28 (7H, m, H_{Ar} and 3H_{Flu}), 7.21-7.11 (6H, m, 2H_{Ar}), 6.86 (2H, d, *J* = 9.3 Hz, H_{Ar}), 2.03-1.85 (4H, m, H_{Bu}), 1.05-0.92 (4H, m, H_{Bu}), 0.57 (6H, t, *J* = 7.3 Hz, H_{Bu}), 0.54-0.44 (4H, m, H_{Bu}). **^{13}C{^{1}H} NMR** (100 MHz, $CDCl_3$) δ = 168.9, 164.7, 153.8, 152.6, 152.3, 148.2, 144.7, 139.0, 132.1, 130.3, 130.2, 129.9, 129.4, 127.6, 127.1, 126.8, 124.5, 123.4, 122.0, 121.4, 121.0, 118.2, 113.8, 112.8, 112.8, 111.9, 85.1, 78.6, 55.8, 39.9, 26.1, 23.0, 13.9. **IR** (KBr, cm^{-1}): *ν* = 3061, 2928 (m, C_{Ar}-H), 2219 (m, C≡N), 1607 (m, C=C), 1586 (s, C=C_{Ar}). **Raman** (neat, cm^{-1}): *ν* = 3066 (vw, C_{Ar}-H), 2221 (s, C≡N), 1609 (s, C=C), 1520 (vs, C=C_{Ar}). **HRMS**: calculated for $C_{47}H_{40}N_5$ $[M+H]^+$ 674.32837, found 674.3278, calculated for $C_{47}H_{39}N_5$ $M^{+\cdot}$ 673.32055, found 673.3197. **UV-vis** (CH_2Cl_2): λ_{max} (log ε) = 274 (4.40), 340 (4.20), 414 (4.53), 489 (4.40).

Synthesis of Fe(η^5-C_5Me_5)(CO)$_2$[C≡C(2-$C_{21}H_{25}$)] (2). In a Schlenk tube under argon, CuI (37 mg, 0.19 mmol, 0.3 eq.) were dissolved in triethylamine (30 mL). After 10 min of stirring, a solution of 2-ethynyl-9,9-dibutyl-9*H*-fluorene (**7**; 194 mg, 0.64 mmol, 1 eq.) in THF (30 mL) was added. The mixture was stirred for 30 min and then a solution of Fe(η^5-C_5Me_5)(CO)$_2$(Cl) (**6**; 200 mg, 0.70 mmol, 1.1 eq.) in THF (30 mL) was added. The reaction mixture was stirred overnight in the dark. After removal of the solvent, the product was extracted with CH_2Cl_2 and filtered through an alumina plug and the filtrate taken to dryness. The compound was dissolved in diethylether, precipitated with *n*-pentane, and subsequent washing with cold methanol and cold *n*-pentane (-50 °C) afforded the title compound as a yellow solid (120 mg, 0.22 mmol, 31 %). **Anal.** Calc for $C_{35}H_{40}O_2Fe$•½CH_2Cl_2: C, 72.15, H 6.99; Found: C, 71.69, H 7.44. **MS** (ESI) m/z 571.2270 $[M+Na]^+$ calc. for $C_{35}H_{40}O_2FeNa$: 571.2270 ($[M+Na]^{+\bullet}$), 543.2324 [M-CO+Na] calc. for $C_{34}H_{40}OFeNa$: 543.2321 ($[M+Na]^{+\bullet}$), 515.2365 [M-2CO+Na] calc. for $C_{33}H_{40}FeNa$: 515.2372 ($[M-2CO+Na]^{+\bullet}$). **^{1}H NMR** (200 MHz, $CDCl_3$): *δ* = 7.78 (s, 1H, H_{flu}), 7.74 (d, 1H, H_{flu}), 7.59-7.75 (m, 2H, H_{flu}), 7.17 (m, 3H, H_{flu}), 1.93 (t, 4H, C$H_{2\text{-}Bu}$), 1.47 (m, 15H, C_5(CH_3)$_5$), 0.90 (m, 8H, C$H_{2\text{-}Bu}$), 0.70 (m, 8H, C$H_{2\text{-}Bu}$), 0.50 (s, 6H, CH_3). **^{13}C{^{1}H} NMR** (125 MHz, C_6D_6): δ = 216.3 (s, *C*O), 151.2 (s, C_{flu}), 151.6 (s, C_{flu}), 151.3 (s, C_{flu}), 142.4 (s, C_{flu}), 138.9 (s, C_{flu}), 131.6 (s, *C*H$_{flu}$), 129.5 (s, C_{flu}), 127.5 (s, *C*H$_{flu}$), 127.2 (s, *C*H$_{flu}$), 126.3 (s, *C*H$_{flu}$), 123.4 (s, *C*H$_{flu}$), 120.3 (s, *C*H$_{flu}$), 120.2 (s, *C*H$_{flu}$), 115.1 (s, Fe*C*≡C), 105.1 (s, FeC≡*C*), 97.4 (s, C_5(CH$_3$)$_5$), 55.6 (s, C_{flu}), 41.2 (s, *C*H$_{2/Bu}$), 26.9 (s, *C*H$_{2/Bu}$), 23.9 (s, *C*H$_{2/Bu}$), 14.4 (s, *C*H$_{2/Bu}$), 10.4 (s, C_5(*C*H$_3$)$_5$). **IR** (KBr/CH_2Cl_2, cm^{-1}): *ν* = 2095/2093 (m, C≡C), 2010/2017 (s, C=O), 1960/1967 (s, C=O).

Synthesis of *trans*-Ru(κ^2-dppe)$_2$[C≡C(2-$C_{21}H_{25}$)](Cl) (3). A mixture of *cis*-Ru(κ^2-dppe)$_2$Cl$_2$ (**8**; 400 mg, 0.41 mmol, 1 eq), 2-ethynyl-9,9-dibutyl-9*H*-fluorene (**7**; 150 mg, 0.50 mmol, 1.2 eq) and $NaPF_6$ (90 mg, 0.5 mmol, 1.2 eq) was stirred 12 h at 35 °C. After filtration and concentration, the solution was poured into Et_2O. The precipitate was filtered and washed several times with Et_2O. The compound was then dissolved in CH_2Cl_2 and Et_3N (3 mL). Subsequently, the volatiles were removed and the product was eluted through a basic alumina plug using CH_2Cl_2 as eluent. After evaporation of the solvent, the title complex was obtained as a yellow solid (313 mg, 0.25 mmol, 61 %). **Anal.** Calc for $C_{75}H_{73}ClRuP_4$: C, 72.95; H, 5.96; Found: C, 72.87; H, 6.06. **MS** (ESI) m/z 1240.4 ($[M-Cl+CH_3CN]^{+\bullet}$, 100 %), calc. for $C_{75}H_{73}P_4Ru$•CH_3CN: 1240.4 ($[M-Cl+CH_3CN]^{+\bullet}$). **^{31}P{^{1}H} NMR** (121 MHz, $CDCl_3$): *δ* = 50.2 (s, P_{dppe}). **^{1}H NMR** (300 MHz, $CDCl_3$): *δ* = 7.51-7.45 (m, 9H, H_{Ar}), 7.41 (d, 1H, $^3J_{H,H}$ = 8.1 Hz, H_{Ar}), 7.22 (m, 11H, H_{Ar}), 7.13 (m, 8H, H_{Ar}), 6.92 (m, 16H, H_{Ar}), 6.59 (m, 2H, H_{Ar}), 2.66 (m, 8H, C$H_{2/dppe}$), 1.89 (m, 4H, C$H_{2/Bu}$), 1.13 (m, 4H, C$H_{2/Bu}$), 0.67 (m, 10H, C$H_{2/Bu}$+ CH_3). **^{13}C{^{1}H} NMR** (125 MHz, $CDCl_3$): *δ* = 151.1 (s, C_{flu}), 150.5 (s, C_{flu}), 142.5 (s, C_{flu}), 137.3 & 136.4 (2 × m, $C_{Ph/dppe}$), 136.7 (s, C_{flu}), 135.1 (2 × s, *C*H$_{Ph/dppe}$), 130.0 (s, C_{flu}), 129.5 (2 × m, *C*H$_{Ph/dppe}$), 129.4 (s, *C*H$_{flu}$), 127.8 & 127.7 (2 × s, *C*H$_{Ph/dppe}$), 127.4 (s, *C*H$_{flu}$), 126.5 (s, *C*H$_{flu}$), 125.0 (quin, $^2J_{C,P}$ = *ca.* 16 Hz, Ru-*C*≡C), 124.8 (s, *C*H$_{flu}$), 123.4 (s, *C*H$_{flu}$), 119.6 (s, *C*H$_{flu}$), 119.5 (s, *C*H$_{flu}$), 115.6 (m, Ru-C≡*C*), 55.4 (s, C_{flu}), 41.4 (s, *C*H$_{2\text{-}flu}$), 31.4 (m, *C*H$_{2/dppe}$), 26.8 (s, *C*H$_{2/flu}$), 24.0 (s, *C*H$_{2/flu}$), 14.7 (s, *C*H$_3$). **IR** (KBr/CH_2Cl_2, cm^{-1}): *ν* = 2065/2066 (s, C≡C).

Synthesis of Ru(κ^2-dppe)$_2$[C≡C(2-$C_{21}H_{25}$)][C≡C(4-$C_6H_4NO_2$)] (4). A mixture of *trans*-Ru(κ^2-dppe)$_2$[C≡C(4-$C_6H_4NO_2$)](Cl) (**9**; 200 mg, 0.18 mmol, 1 eq.), 2-ethynyl-9,9-dibutyl-9*H*-fluorene (**7**; 73 mg, 0.24 mmol, 1.3 eq.), $NaPF_6$ (47 mg, 0.28 mmol, 1.5 eq.) and 5 drops of Et_3N were stirred 12 h at reflux. The solvents were removed and the compound was filtered through a deactivated alumina plug and eluted with a petroleum spirit/dichloromethane mixture (1:2 to 2:1). After removal of the volatiles, the product was washed with petroleum spirit (3 x 20 mL) to afford the

title compound as a red solid (218 mg, 0.16 mmol, 90 %). **Anal.** Calc for $C_{83}H_{77}NO_2P_4Ru$: C, 74.09; H, 5.77; N, 1.04, Found: C, 73.96; H, 5.89; N, 1.10. **MS** (ESI) m/z 1384.7 ([M+K]$^{+\bullet}$, 100 %), 1368.7 ([M+Na]$^{+\bullet}$, 60 %), calc. for $C_{67}H_{68}FeP_2K$: 1384.4. **^{31}P{^{1}H} NMR** (121 MHz, $CDCl_3$): δ = 53.2 (s, P_{dppe}). **^{1}H NMR** (400 MHz, CD_2Cl_2): δ = 8.01 (d, 2H, $^3J_{H,H}$ = 9.0 Hz, H_{Ar}), 7.71 (m, 8H, H_{Ar}), 7.67 (m, 1H, $^3J_{H,H} \approx$ 7.5 Hz, H_{flu}),7.56 (dd, 1H, $^3J_{H,H}$ = 7.8 Hz, $^5J_{H,H}$ = 0.4 Hz, H_{flu}), 7.40-7.33 (m, 10H, H_{Ar}), 7.30 (dd, 1H, $^3J_{H,H}$ = 7.3 Hz, $^4J_{H,H}$ = 1.2 Hz, H_{flu}), 7.27-7.21 (m, 8H, H_{Ar}), 7.06-6.97 (m, 16H, H_{Ar}), 6.92 (dd, 1H, $^3J_{H,H}$ = 7.8 Hz, $^4J_{H,H}$ = 1.2 Hz, H_{flu}), 6.90 (s, 1H, H_{flu}), 6.67 (d, 2H, $^3J_{H,H}$ = 9.0 Hz, H_{Ar}), 2.71 (m, 8H, $CH_{2/dppe}$), 1.93 (m, 4H, $CH_{2/Bu}$), 1.22 (m, 4H, $CH_{2/Bu}$), 0.79 (t, 6H, $^3J_{H,H}$ = 7.3 Hz, $CH_{3/Bu}$), 0.69 (m, 4H, $CH_{2/Bu}$). **^{13}C{^{1}H} NMR** (125 MHz, $CDCl_3$): δ = 155.0 (quin, $^2J_{C,P}$ = *ca.* 15 Hz, Ru-*C*≡C), 151.4 (s, C_{flu}), 150.7 (s, C_{flu}), 143.3 (s, C_{Ar}), 142.4 (s, C_{flu}), 138.1 (s, C_{Ar}), 137.4 & 137.2 (2 × m + s, $C_{Ph/dppe}$+C_{flu}), 135.1 & 134.6 (2 × s, $CH_{Ph/dppe}$), 130.6 (CH_{Ar}), 129.9 (s, C_{flu}), 129.5 (2 × m, $CH_{Ph/dppe}$), 129.2 (s, CH_{flu}), 127.9 (2 × s, $CH_{Ph/dppe}$), 127.4 (s, CH_{flu}), 126.7 (s, CH_{flu}), 124.8 (s, CH_{flu}), 124.1 (s, CH_{Ph}), 123.3 (s, CH_{flu}), 120.1 (m, Ru-C≡*C*), 119.7 (s, 2CH_{flu}), 119.6 (m, Ru-C≡*C*), 55.4 (s, C_{flu}), 41.4 (s, $CH_{2/flu}$), 32.1 (m, $CH_{2/dppe}$), 26.8 (s, $CH_{2/flu}$), 24.0 (s, $CH_{2/flu}$), 14.7 (s, CH_3), Ru-*C*≡C (C_α) not detected. **IR** (KBr/CH_2Cl_2, cm^{-1}): ν = 2070 (sh), 2051/2046 (s, C≡C), 1579/1581 (s, $NO_2[\nu_{as}]$), 1324/1323 (s, $NO_2[\nu_{sym}]$).

Synthesis of [Fe(η^5-C_5Me_5)(κ^2-dppe)[C≡C(4-C_5H_4N{CH_2(2-$C_{13}H_9$)})]] [PF_6] (5[PF_6]). In a Schlenk tube under argon, Fe(η^5-C_5Me_5)(κ^2-dppe)[C≡C(4-C_5H_4N)}] (**10**; 300 mg, 0.43 mmol, 1 eq) and 2-bromomethylfluorene (**11**; 110 mg, 0.42 mmol, 0.98 eq) were stirred for 12 h in THF at room temperature. To this mixture, potassium hexafluorophosphate (88 mg, 0.48 mmol, 1.1 eq) was added and the reaction was stirred for a further 5 h. The solvent was then removed and the deep blue product was extracted with dichloromethane. After removal of the solvent, the compound was precipitated in a mixture of toluene and *n*-pentane. The solid was then washed with *n*-pentane (2 x 50 mL) to afford the title complex as a deep blue solid (337 mg, 0.33 mmol, 79 %). **Anal.** Calc for $C_{57}H_{54}F_6FeNP_3$•½CH_2Cl_2: C, 65.26; H, 5.24; N, 1.32; Found C, 65.72; H, 5.44; N, 1.34. **MS** (ESI) m/z 870.3088 (M$^{+\bullet}$) calc. for $C_{57}H_{54}FeNP_2$: 870.3081 (M$^{+\bullet}$). **^{31}P{^{1}H} NMR** (81 MHz, $CDCl_3$): δ = 98.1 (s, P_{dppe}), -142.9 (sept, $^1J_{P,F}$ = 713 Hz, PF_6^-). **^{1}H NMR** (200 MHz, $CDCl_3$): δ = □□□□□□d□□$^3J_{H,H}$ = 6.6 Hz,□□H, H_{Py}□□□□□□□□□m, 3H, H_{flu}), 7.57 (m, 8H, $H_{Ph/dppe}$+ H_{flu}), 7.49-7.20 (m, 16H, $H_{Ph/dppe}$), 6.59 (d, 2H, $^3J_{H,H}$ = 6.6 Hz, 2H, H_{Py}), 5.30 (s, 2H, CH_2), 3.95 (s, 2H, CH_2), 2.63 (m, 2H, $CH_{2/dppe}$), 2.13 (m, 2H, $CH_{2/dppe}$), 1.43 (s, 15H, $C_5(CH_3)_5$). **^{13}C{^{1}H} NMR** (100 MHz, CD_2Cl_2): δ = 144.7 (s, C_{flu}), 143.7 (s, C_{flu}), 143.0 (s, C_{flu}), 140.5 (s, C_{flu}), 139.7 (s, CH_{Py}), 137.0-135, (2 × m; $C_{Ph/dppe}$), 133.6 & 133.3 (2 × m, $CH_{Ph/dppe}$), 131.8 (s, CH_{flu}), 130.7 (t, $^2J_{C,P}$ = *ca.* 6.4 Hz, C_{Py}), 130.0 & 129.6 (2 × s, $CH_{Ph/dppe}$), 127.9 & 127.9 (s, $CH_{Ph/dppe}$), 127.5 (s, CH_{flu}), 127.3 (s, C_{flu}), 126.9 (s, CH_{flu}), 126.4 (s, CH_{Py}), 125.3 (s, CH_{flu}), 125.2 (s, CH_{flu}), 120.6 (s, CH_{flu}), 120.2 (s, CH_{flu}), 91.6 (s, $C_5(CH_3)_5$), 62.2 (s, NCH_2), 36.8 (s, $CH_{2/flu}$), 30.3 (m, $CH_{2/dppe}$), 9.8 (s, $C_5(CH_3)_5$, [Ru-*C*≡C (C_α), Ru-C≡*C* (C_β) not detected]. **IR** (KBr/CH_2Cl_2, cm^{-1}): ν = 1987/1988 (s, C≡C), 1619/1620 (s, Py), 842/847 (s, P-F).

Luminescence measurements. The samples used to make the solutions were freshly recrystallized or thoroughly washed with cooled ether / pentane to remove any organic impurity prior to the measurements. Luminescence measurements in solution were performed in dilute deoxygenated solutions (except in the case of compound **12**[PF_6]) contained in air-tight quartz cells of 1 cm pathlength (*ca.* 10^{-6} M, optical density < 0.1) at room temperature (298 K). Fully corrected excitation and emission spectra were obtained with an optical density at $\lambda_{exc} \leq$ 0.1 to minimize internal absorption. Luminescence quantum yields were measured according to literature procedures.[59] UV-vis absorption spectra used for the calculation of the luminescence quantum yields were recorded using a double beam Jasco V-570 spectrometer.

Spectroelectrochemistry. Solution UV-Vis-NIR spectra of the oxidized species were obtained at 243 K or 298 K by electrogeneration on a platinum mesh electrode in a 0.05 mm optically transparent thin-layer electrochemical (OTTLE) cell,[60] using a silver wire as pseudo-reference and a platinum wire as counter-electrode. Solutions were made up with 0.20 M [*n*-Bu_4N][PF_6] in dry and deoxygenated CH_2Cl_2, and were kept under an atmosphere of pure nitrogen.

Z-scan Measurements. Third-order nonlinear optical properties were investigated as previously described,[61] but with some modifications. The laser system consisted of a Quantronix Integra-C3.5F pumping a Quantronix Palitra-FS optical parametric amplifier, tuneable over a wavelength range from 500 nm to 2000 nm. The output wavelength was confirmed by use of an Ocean Optics USB2000+ spectrometer (500-1000 nm) or an Ocean Optics NIR-Quest spectrometer (1000-1800 nm). The system delivered 130 fs pulse with a 1 kHz repetition rate. Colored glass filters and a Thorlabs polarizing filter were used to remove unwanted wavelengths and the power adjusted by use of neutral density filters, attenuating it to the μJ/pulse range to obtain nonlinear phase shifts between 0.2 to 1.3 rad. The focal length of the lens used in the experiment was 75 mm, which gave 25-40 μm beam waists resulting in Rayleigh lengths sufficiently longer than that of the sample thickness that a "thin-sample" assumption was justified. Solutions of compounds in "as received" CH_2Cl_2 (see text), deoxygenated and distilled CH_2Cl_2, or deoxygenated and distilled THF, of 0.1 w/w% concentration in 1 mm glass cells were analyzed. Samples travelled down the Z-axis on a Thorlabs motorized stage between -20 and 20 mm (where 0 was the laser focus). Data were collected by three Thorlabs photodiodes, 500-900 nm with Si based detectors, 900-1300 nm with InGaAs detectors and 1300-2000 nm with amplified InGaAs detectors, monitoring the laser input, the open-aperture signal and the closed-aperture signal. Data from the detectors were fed into three channels of a Tektronix digital oscilloscope, collected with a custom LabVIEW program, and fitted with theoretical traces with a program that used equations derived by Sheik-Bahae *et al.*[62] A sample of the solvent was run at each wavelength to account for solvent and cell contribution to the Z-scan signals and the light intensity was determined from a Z-scan run on a 3 mm fused silica plate; the real and imaginary components of the second hyperpolarizability (γ) of the materials were calculated assuming additivity of the nonlinear contributions of the solvent and the solute and the applicability of the Lorentz local field approximation. The values of the imaginary parts of γ were also converted into values of the two-photon absorption cross-sections σ_2.

Crystallography. Data collection of crystals of **4** and **12**[PF_6] were performed on an Oxford Diffraction Xcalibur Saphir 3 diffractometer or an image plate APEXII Bruker-AXS spectrometer at 150 K, with graphite monochromatized MoK_α radiation. The cell parameters (ESI) were obtained with Denzo and Scalepack.[63] The data collection[64] provided reflections from which the independent reflections were obtained after data reduction using Denzo and Scalepack.[63] The structures were solved with SIR-97 which revealed the non-hydrogen atoms.[65] After anisotropic refinement, the remaining atoms were found in Fourier difference maps. The complete structures were then refined with SHELXL97[66] by the full-matrix least-square technique. Atomic scattering factors were taken from the literature.[67]

Computational Details. Calculations were performed using the Amsterdam Density Functional (ADF) program,[68] version ADF2012. Scalar relativistic effects were treated via the Zeroth-Order Regular Approximation (ZORA) method.[69] In all calculations, all-electron Triple Zeta plus Polarization (TZP) Slater orbital basis sets were used for all atoms. Geometry optimizations were undertaken with suitable symmetry constraints using the exchange-correlation (XC) functional and the Generalized Gradient Approximation (GGA) proposed by Becke and Perdew (BP).[70] The model systems were simplified by using 1,2-bis(dimethylphosphino)methane (dmpm) ligand instead of 1,2-bis(diphenylphosphino) ethane (dppe) and hydrogen instead of methyl in the butyl groups. UV-Vis spectra were calculated using the Statistical Average of Orbital Potentials (SAOP) functional[71] with the same TZP basis sets.

Acknowledgements

Partial Funding for the project was obtained from the "Université Européenne de Bretagne" (UEB) and from FEDER by an EPT grant in the "MITTSI" program from RTR BRESMAT. The CNRS (PICS program N° 5676 and 7106) are acknowledged for financial support. F.P. and G.G. thank the CNRS for financial support and Region Bretagne for a Ph.D. grant. F.M. thanks the MENRT for a doctoral grant. M.G.H. thanks the Australian Research Council (ARC) for financial support and M.P.C. thanks the ARC for an Australian Research Fellowship.

Keywords: Metal-Alkynyl Complex • Nonlinear Optical Properties • Two-Photon Absorption • Luminescence • Electrochemistry

[1] See for instance: a) M. Pawlicki, H. A. Collins, R. G. Denning and H. L. Anderson, *Angew. Chem. Int. Ed.* **2009**, *48*, 3244-3266; b) W.-Y. Wong, *Coord. Chem. Rev.* **2005**, *249*, 971-997; c) V. Balzani, A. Credi and M. Venturi, *Chem. Eur. J.* **2002**, *8*, 5525-5532; d) V. W.-W. Yam, K. K.-W. Lo and K. M.-C. Wong, *J. Organomet. Chem.* **1999**, *578*, 3-30; e) R. Ziessel, *Synthesis* **1999**, 1839-1865.

[2] V. Balzani and A. P. de Silva, *Electron Transfer in Chemistry*, Wiley-VCH, **2000**, p.

[3] a) S. Marques-Gonzalez, M. Parthey, D. S. Yufit, J. A. K. Howard, M. Kaupp and P. J. Low, *Organometallics* **2014**, *33*, 4947-4963; b) A. Vacher, F. Barrière and D. Lorcy, *Organometallics* **2013**, ASAP; c) M. Akita and T. Koike, *J. Chem. Soc., Dalton Trans.* **2008**, 3523-3530; d) S. Rigaut, D. Touchard and P. H. Dixneuf in *Redox active architectures and carbon-rich ruthenium complexes as models for molecular wires*, *Vol.* (Ed. T. Hirao), Springer Verlag, Heidelberg, **2006**; e) T. Ren, *Organometallics* **2005**, *24*, 4854-4870; f) P. J. Low, *J. Chem. Soc., Dalton Trans.* **2005**, 2821-2824; g) F. Paul and C. Lapinte, *Coord. Chem. Rev.* **1998**, *178/180*, 431-509.

[4] a) N. Robertson and G. A. McGowan, *Chem. Soc. Rev.* **2003**, *32*, 96-103; b) R. L. Caroll and C. B. Gorman, *Angew. Chem., Int. Ed. Engl.* **2002**, *41*, 4379-4400.

[5] a) S. Lyu, Y. Farré, L. Ducasse, Y. Pellegrin, T. Toupance, C. Olivier and F. Odobel, *RSC Adv.* **2016**, *6*, 19928-19936; b) S. De Sousa, S. Lyu, L. Ducasse, T. Toupance and C. Olivier, *J. Mater. Chem. A* **2015**, *3*, 18256-18264; c) S. De Sousa, L. Ducasse, B. Kauffmann, T. Toupance and C. Olivier, *Chem. Eur. J.* **2014**, *20*, 7017-7024.

[6] a) M. Srebro, E. Anger, I. B. Moore, N. Vanthuyne, C. Roussel, R. Réau, J. Autschbach and J. Crassous, *Chem. Eur. J.* **2015**, *21*, 17100-17115; b) E. Anger, M. Srebro, N. Vanthuyne, L. Toupet, S. Rigaut, C. Roussel, J. Autschbach, J. Crassous and R. Réau, *J. Am. Chem. Soc.* **2012**, *134*, 15628-15630

[7] a) G. Grelaud, M. P. Cifuentes, F. Paul and M. G. Humphrey, *J. Organomet. Chem.* **2014**, *751*, 181-200; b) R. L. Roberts, T. Schwich, T. C. Corkery, M. P. Cifuentes, K. A. Green, J. D. Farmer, P. J. Low, T. B. Marder, M. Samoc and M. G. Humphrey, *Adv. Mat.* **2009**, *21*, 2318-2322; c) M. Samoc, J.-P. Morrall, G. T. Dalton, M. P. Cifuentes and M. G. Humphrey, *Angew. Chem. Int. Ed.* **2007**, *46*, 731-733; d) M. P. Cifuentes, M. G. Humphrey, J. P. Morrall, M. Samoc, F. Paul, T. Roisnel and C. Lapinte, *Organometallics* **2005**, *24*, 4280-4288; e) J. P. Morrall, G. T. Dalton, M. G. Humphrey and M. Samoc, *Adv. Organomet. Chem.* **2008**, *55*, 61-136; f) N. J. Long and C. K. Williams, *Angew. Chem., Int. Ed. Engl.* **2003**, *42*, 2586-2617; g) C. E. Powell and M. G. Humphrey, *Coord. Chem. Rev.* **2004**, *248*, 725-756.

[8] a) A. Merhi, X. Zhang, D. Yao, S. Drouet, O. Mongin, F. Paul, J. A. G. Williams, M. A. Fox and C. O. Paul-Roth, *Dalton Trans.* **2015**, *44*, 9470-9485; b) L. Norel, E. Di Piazza, M. Feng, A. Vacher, X. He, T. Roisnel, O. Maury and S. Rigaut, *Organometallics* **2014**, *33* 4824−4835; c) M. Murai, M. Sugimoto and M. Akita, *Dalton Transactions* **2013**, *42*, 16108-16120; d) E. Di Piazza, L. Norel, K. Costuas, A. Bourdolle, O. Maury and S. Rigaut, *J. Am. Chem. Soc.* **2011**, *133*, 6174-6775; e) F. de Montigny, G. Argouarch, T. Roisnel, L. Toupet, C. Lapinte, S. C.-F. Lam, C.-H. Tao and V. W.-W. Yam, *Organometallics* **2008**, *27*, 1912-1923; f) K. M.-C. Wong, S. C.-F. Lam, C.-C. Ko, N. Zhu, V. W.-W. Yam, S. Roué, C. Lapinte, S. Fathallah, K. Costuas, S. Kahlal and J.-F. Halet, *Inorg. Chem.* **2003**, *42*, 7086-7097.

[9] M. E. Smith, E. L. Flynn, M. A. Fox, A. Trottier, E. Werde, D. S. Yufit, J. A. K. Howard, K. L. Ronayne, M. Towrie, A. W. Parker, F. Hartl and P. J. Low, *Chem. Commun.* **2008**, 5845-5847.

[10] G. S. He, L.-S. Tan, Q. Zheng and P. N. Prasad, *Chem. Rev.* **2008**, *108*, 1245-1330.

[11] F. Malvolti, C. Rouxel, A. Triadon, G. Grelaud, N. Richy, O. Mongin, M. Blanchard-Desce, L. Toupet, F. I. Abdul Razak, R. Stranger, M. Samoc, X. Yang, G. Wang, A. Barlow, M. P. Cifuentes, M. G. Humphrey and F. Paul, *Organometallics* **2015**, *34*, 5418–5437.

[12] a) D. Astruc, *Electron Transfer and Radical Processes in Transition-Metal Chemistry*, VCH Publishers, Inc., New York, Weinheim, Cambridge, **1995**, p; b) R. A. Marcus and N. Sutin, *Biochim. Biophys. Acta* **1985**, *811*, 265-322.

[13] a) J. Chatt and R. G. Hayter, *J. Chem. Soc.* **1961**, 896-904; b) D. Touchard, P. Haquette, S. Guesmi, L. Le Pichon, A. Daridor, L. Toupet and P. H. Dixneuf, *Organometallics* **1997**, *16*, 3640-3648.

[14] a) N. Gauthier, N. Tchouar, F. Justaud, G. Argouarch, M. P. Cifuentes, L. Toupet, D. Touchard, J.-F. Halet, S. Rigaut, M. G. Humphrey, K. Costuas and F. Paul, *Organometallics* **2009**, *28*, 2253-2266; b) M. A. Fox, J. E. Harris, S. Heider, V. Pérez-Gregorio, M. E. Zakrzewska, J. D. Farmer, D. S. Yufit, J. A. K. Howard and P. J. Low, *J. Organomet. Chem.* **2009**, *694*, 2350-2358.

[15] a) M. Younus, N. J. Long, P. R. Raithby, J. Lewis, N. A. Page, A. J. P. White, D. J. Williams, M. C. B. Colbert, A. J. Hodge, M. S. Khan and D. G. Parker, *J. Organomet. Chem.* **1999**, *578*, 198-209; b) S. K. Hurst, M. P. Cifuentes, J. P. L. Morrall, N. T. Lucas, I. R. Whittall, M. G. Humphrey, I. Asselberghs, A. Persoons, M. Samoc, B. Luther-Davies and A. C. Willis, *Organometallics* **2001**, *20*, 4664-4675; c) For mono-alkynyl complexes, see also: J. P. Morrall, M. P. Cifuentes, M. G. Humphrey, R. Kellens, E. Robijns, I. Asselberghs, K. Clays, A. Persoons, M. Samoc and A. C. Willis, *Inorg. Chim. Acta* **2006**, *359*, 998-1005; d) 02.

[16] a) The molecular peak of these complexes could not be detected by ESI-MS, but a cationic adduct of the complex formed after exchange of the chloride with acetonitrile was detected for **3**, while potassium and sodium adducts of the complex were detected for **4**; b) In the ^{13}C NMR spectrum, only one of the two diagnostic quintets expected for $C_{\square}$ acetylide carbon atoms coupled to four phosphorus atoms could be plainly detected. The weak signal of the second $C_{\square}$ carbon atom is certainly hidden by the other signals in the aromatic range.

[17] A. M. McDonagh, M. P. Cifuentes, I. R. Whittall, M. G. Humphrey, M. Samoc, B. Luther-Davies and D. C. R. Hockless, *J. Organomet. Chem.* **1996**, *526*, 99-103.

[18] For mono-alkynyl complexes, see also: F. Paul, B. J. Ellis, M. I. Bruce, L. Toupet, T. Roisnel, K. Costuas, J.-F. Halet and C. Lapinte, *Organometallics* **2006**, *25*, 649-665.

[19] F. H. Allen, O. Kennard, D. G. Watson, L. Brammer, A. G. Orpen and R. Taylor, *J. Chem. Soc., Perkin Trans.* **1987**, *2*, S1-S19.

[20] S. Le Stang, F. Paul and C. Lapinte, *Inorg. Chim. Acta* **1999**, *291*, 403-425.

[21] S. Le Stang, D. Lenz, F. Paul and C. Lapinte, *J. Organomet. Chem.* **1998**, *572*, 189-192.

[22] F. Paul, J.-Y. Mevellec and C. Lapinte, *J. Chem. Soc., Dalton Trans.* **2002**, 1783-1790.

[23] K. Costuas, F. Paul, L. Toupet, J.-F. Halet and C. Lapinte, *Organometallics* **2004**, *23*, 2053-2068.

[24] A. Weller, *Z. Phys. Chem. N. F.* **1982**, *133*, 93-98.

[25] In this equation, e is the electron charge, ε_0 is the dielectric constant in vacuum, ε is the relative dielectric constant and a is the distance between the positive and negative charge in the CT state. The a values were estimated from the distance between the metal center and the midpoint of the fluorene unit for **1**, **3** and **4** or the nitrogen atom for **5**[PF_6] and **12**[PF_6], the distances being obtained/approximated for **1**, **3**, **4**, **5**[PF_6] and **12**[PF_6] from the available X-ray data for **1**,[11] **4**, **9**[26] and **12**[PF_6].

[26] F. Paul, *work in progress*.

[27] C. Poriel, J.-J. Liang, J. Rault-Berthelot, F. Barrière, N. Cocherel, A. M. Z. Slawin, D. Horhant, M. Virboul, G. Alcaraz, N. Audebrand, L. Vignau, N. Huby, G. Wantz and L. Hirsch, *Chem. Eur. J.* **2007**, *13*, 10055 – 10069.

[28] R. Denis, L. Toupet, F. Paul and C. Lapinte, *Organometallics* **2000**, *19*, 4240-4251.

[29] F. Paul and G. Argouarch, *work in progress*.

[30] M. Akita, M. Terada, S. Oyama and Y. Moro-Oka, *Organometallics* **1990**, *9*, 816-825.

[31] See for instance: a) G. Argouarch, G. Grelaud and F. Paul, *Organometallics* **2010**, *29*, 4414-4416, and refs therein; b) M. Sato, Y. Hayashi, S. Kumakura, N. Shimizu, M. Katada and S. Kawata,

Organometallics **1996**, *15*, 721-728; c) S. Nakanishi, K.-I. Goda, S.-I. Uchiyama and Y. Otsuji, *Bull. Chem. Soc. Jpn* **1992**, 2560-2561.
[32] N. Gauthier, C. Olivier, S. Rigaut, D. Touchard, T. Roisnel, M. G. Humphrey and F. Paul, *Organometallics* **2008**, *27*, 1063-1072.
[33] B. Babgi, L. Rigamonti, M. P. Cifuentes, T. C. Corkery, M. D. Randles, T. Schwich, S. Petrie, R. Stranger, A. Teshome, I. Asselberghs, K. Clays, M. Samoc and M. G. Humphrey, *J. Am. Chem. Soc.* **2009**, *131*, 10293–10307.
[34] F. Paul and F. Malvolti, *work in progress*.
[35] F. Paul, K. Costuas, I. Ledoux, S. Deveau, J. Zyss, J.-F. Halet and C. Lapinte, *Organometallics* **2002**, *21*, 5229-5235.
[36] F. Paul and O. Cador, *work in progress*.
[37] N. I. Nijegorodov and W. S. Downey, *J. Phys. Chem.* **1994**, *98*, 5639-5643.
[38] Fluorescence originating from an excimer is possibly detected for that compound (see ESI), since a second emission band at very low energy is also seen.
[39] See for instance: a) M. Matsui, K. Ooiwa, A. Okada, Y. Kubota, K. Funabiki and H. Sato, *Dyes and Pigments* **2013**, *99*, 916-923; b) I. Richter, M. R. Warren, J. Minari, S. A. Elfeky, W. Chen, M. F. Mahon, P. R. Raithby, T. D. James, K. Sakurai, S. J. Teat, S. D. Bull and J. S. Fossey, *Chem. Asian J.* **2009**, *4*, 194-198.
[40] a) Y. Nakano, J. Komiyama and T. Iijima, *Coll. Polym. Sci.* **1987**, *265*, 139-147; b) M. Shinitzky and B. Rivnay, *Biochemistry* **1977**, *16*, 982-986.
[41] C. E. Powell, M. P. Cifuentes, J. P. Morrall, R. Stranger, M. G. Humphrey, M. Samoc, B. Luther-Davies and G. A. Heath, *J. Am. Chem. Soc.* **2003**, *125*, 602-610.
[42] K. Costuas and S. Rigaut, *Dalton Trans.* **2011**, *40*, 5643-5658.
[43] This phenomenon is not to be confused with dual luminescence, more frequently encountered in solution at ambient temperature and for which fluorescence and phosphorescence are simultaneously observed, as happens when the metallic ion promotes efficient intersystem crossing of the emissive singlet state to a triplet state via its spin-orbit coupling.[45]
[44] K.-Y. Kim, A. H. Shelton, M. Drobizhev, N. Makarov, A. Rebane and K. S. Schanze, *J. Phys. Chem. A* **2010**, 7003–7013.
[45] a) F. Geist, A. Jackel and R. F. Winter, *Dalton Trans.* **2015**, *44*, 3974-3987, and refs therein; b) D. N. Kozhevnikov, V. N. Kozhevnikov, M. Z. Shafikov, A. M. Prokhorov, D. W. Bruce and J. A. G. Williams, *Inorg. Chem.* **2011**, *50*, 3804–3815; c) R. Westlund, E. Glimsdal, M. Lindgren, R. Vestberg, C. Hawker, C. Lopes and E. Malmstrom, *J. Mater. Chem.* **2008**, *18*, 166-175; d) J. E. Rogers, J. E. Slagle, D. M. Krein, A. R. Burke, B. C. Hall, A. Fratini, D. G. McLean, P. A. Fleitz, T. M. Cooper, M. Drobizhev, N. S. Makarov, A. Rebane, K.-Y. Kim, R. Farley and K. S. Schanze, *Inorg. Chem.* **2007**, *46*, 6483-6494; e) J. van Slageren, R. F. Winter, A. Klein and S. Hartmann, *J. Organomet. Chem.* **2003**, *670*, 137-143.
[46] S. J. Stickler and R. A. Berg, *J. Chem. Phys.* **1962**, *37*, 814-822.
[47] The match is poorer for **1**, possibly because of a larger structural reorganization.
[48] J.-F. Halet and C. Lapinte, *Coord. Chem. Rev.* **2013**, *257*, 1584-1613.
[49] In eq. 3, k_b is the Boltzman constant and T the temperature, while $C = (\pi/\hbar^2 k_B T \lambda)^{1/2}$ is a fairly constant term for **1**, **3** and **4**.
[50] a) F. Paul, G. da Costa, A. Bondon, N. Gauthier, S. Sinbandhit, L. Toupet, K. Costuas, J.-F. Halet and C. Lapinte, *Organometallics* **2007**, *26*, 874-896; b) S. Ibn Ghazala, F. Paul, L. Toupet, T. Roisnel, P. Hapiot and C. Lapinte, *J. Am. Chem. Soc.* **2006**, *128*, 2463-2476.
[51] For **5**[PF_6] higher values for $\Delta G^{\neq}$ of 0.0361 eV and 0.1137 eV were found for the reductive- and oxidative-quenching pathways of the LC state (ESI).
[52] Energy transfer[53] or intersystem crossing[45e] have also been sometimes envisioned to rationalize the low fluorescence yields of related carbon-rich Ru(II) complexes.
[53] a) R. Gatri, I. Ouerfelli, M. L. Efrit, F. Serein-Spirau, J.-P. Lère-Porte, P. Valvin, T. Roisnel, S. Bivaud, H. Akdas-Kilig and J.-L. Fillaut, *Organometallics* **2014**, *33*, 665−676; b) A. Vacher, F. Barrière, F. Camerel, J.-F. Bergamini, T. Roisnel and D. Lorcy, *Dalton Trans.* **2013**, *42*, 383-394.
[54] μ_{gg} is the ground state dipole moment, μ_{ee} is an excited state dipole moment, $\mu_{ee'}$ and μ_{ge} are transition dipole moments, and E_{ge} and $E_{ge'}$ are optical absorption energies.
[55] M. P. Cifuentes, C. E. Powell, J. P. L. Morrall, A. M. McDonagh, N. T. Lucas, M. G. Humphrey, M. Samoc, S. Houbrechts, I. Asselberghs, K. Clays, A. Persoons and T. Isoshima, *J. Am. Chem. Soc.* **2006**, *128*, 10819-10832.
[56] K. A. Green, M. P. Cifuentes, M. Samoc and M. G. Humphrey, *Coord. Chem. Rev.* **2011**, *255*, 2530-2541.
[57] M. Akita, M. Terada, M. Tanaka and Y. Moro-Oka, *J. Organomet. Chem.* **1996**, *510*, 255-261.
[58] S. Drouet and C. O. Paul-Roth, *Tetrahedron* **2009**, *65*, 10693-10700.
[59] a) N. Demas and G. A. Crosby, *J. Phys. Chem.* **1971**, *75*, 991-1024; b) D. F. Eaton, *Pure Appl. Chem.* **1988**, *60*, 1107-1114.
[60] C. M. Duff and G. A. Heath, *Inorg. Chem.* **1991**, *30*, 2528-2535.
[61] A. Merhi, G. Grelaud, N. Ripoche, A. Barlow, M. P. Cifuentes, M. G. Humphrey, F. Paul and C. O. Paul-Roth, *Polyhedron* **2015**, *86*, 64-70.
[62] M. Sheikh-Bahae, A. A. Said, T. Wei, D. J. Hagan and E. W. van Stryland, *IEEE J. Quant. Electr.* **1990**, *26*, 760-769.
[63] Z. Otwinowski and W. Minor in *Processing of X-ray diffraction data collected in oscillation mode*, *Vol. 276* Eds.: C. W. Carter and R. M. Sweet), Academic Press, London, **1997**, pp. 307-326.
[64] Nonius B. V., *Kappa CCD Software*, Delft, The Netherlands, **1999**, p.
[65] A. Altomare, J. Foadi, C. Giacovazzo, A. Guagliardi, A. G. G. Moliterni, M. C. Burla and G. Polidori, *J. Applied Cryst.* **1998**, *31*, 74-77.
[66] G. M. Sheldrick, *SHELX97-2. Program for the refinement of crystal structures*, Univ. of Göttingen, Germany, **1997**, p.
[67] D. Reidel, *International Tables for X-ray Crystallography*, Kynoch Press (present distrib. D. Reidel, Dordrecht), Birmingham, **1974**, p.
[68] E. J. Baerends, T. Ziegler, J. Autschbach, D. Bashford, A. Bérces, F. M. Bickelhaupt, C. Bo, P. M. Boerrigter, L. Cavallo, D. P. Chong, L. Deng, R. M. Dickson, D. E. Ellis, M. van Faassen, L. Fan, T. H. Fischer, C. Fonseca Guerra, A. Ghysels, A. Giammona, S. J. A. van Gisbergen, A. W. Götz, J. A. Groeneveld, O. V. Gritsenko, M. Grüning, S. Gusarov, F. E. Harris, P. van den Hoek, C. R. Jacob, H. Jacobsen, L. Jensen, J. W. Kaminski, G. van Kessel, F. Kootstra, A. Kovalenko, M. V. Krykunov, E. van Lenthe, D. A. McCormack, A. Michalak, M. Mitoraj, J. Neugebauer, V. P. Nicu, L. Noodleman, V. P. Osinga, S. Patchkovskii, P. H. T. Philipsen, D. Post, C. C. Pye, W. Ravenek, J. I. Rodríguez, P. Ros, P. R. T. Schipper, G. Schreckenbach, J. S. Seldenthuis, M. Seth, J. G. Snijders, M. Solà, M. Swart, D. Swerhone, G. te Velde, P. Vernooijs, L. Versluis, L. Visscher, O. Visser, F. Wang, T. A. Wesolowski, E. M. van Wezenbeek, G. Wiesenekker, S. K. Wolff, T. K. Woo and A. L. Yakovlev in *ADF2012*, *Vol.* Theoretical Chemistry, Vrije Universiteit, Amsterdam, The Netherlands, **2012**.
[69] E. V. Lenthe, A. E. Ehlers and E. J. Baerends, *J. Chem. Phys.* **1999**, *110*, 8943-8953.
[70] a) A. D. Becke, *Phys. Rev. A.* **1988**, *38*, 3098-3100; b) J. P. Perdew, *Phys. Rev. B* **1986**, *33*, 8822-8824; c) J. P. Perdew, *Phys. Rev. B* **1986**, *34*, 7406.
[71] O. V. Gritsenko, P. R. T. Schipper and E. J. Baerends, *Chem. Phys. Lett.* **1999**, *302*, 199-207.

Entry for the Table of Contents

FULL PAPER

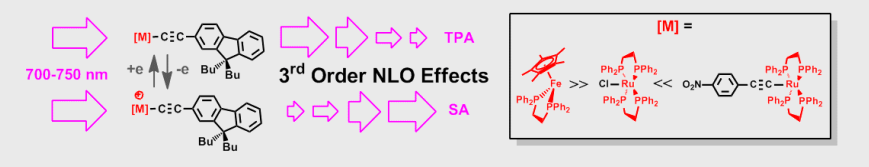

The linear and third-order nonlinear optical properties of a series of new 2-ethynylfluorene complexes are investigated and compared to those of known Fe(Cp*)(dppe) analogues. Among these, the bis-alkynyl Ru(II) derivatives give rise to remarkably large and potentially redox-switchable apparent two-photon absorption in the 700-750 nm wavelength range.

Floriane Malvolti, Cedric Rouxel, Guillaume Grelaud, Loic Toupet, Thierry Roisnel, Adam Barlow, Fazira I. Abdul Razak, Robert Stranger, Marie P. Cifuentes, Mark G. Humphrey, Olivier Mongin, Mireille Blanchard-Desce, Christine Paul-Roth and Frédéric Paul**

Page No. – Page No.

Iron and Ruthenium Alkynyl Complexes with 2-Fluorenyl Groups: Some Linear and Nonlinear Optical Absorption Properties